BULLETIN OF CANADIAN PETROLEUM GEOLOGY
VOL. 58, NO. 1 (MARCH, 2010), P. 17–35

Lower Paleozoic foreland basins in eastern Canada: tectono-thermal events recorded by faults, fluids and hydrothermal dolomites

DENIS LAVOIE
Geological Survey of Canada
Québec Division
490 de la Couronne
Québec City, QC G1K 9A9
delavoie@nrcan.gc.ca

GUOXIANG CHI
Department of Geology
University of Regina
3737 Wascana Parkway
Regina, SK S4S 0A2
guoxiang.chi@uregina.ca

ABSTRACT

Dolomites in Lower and Middle Ordovician and Lower Silurian carbonates in Anticosti and Gaspé, respectively, are documented petrographically and geochemically to originate from early replacement and later void-filling phases, both derived from high temperature brines. These dolomite-rich intervals are interpreted as hydrothermal dolomites that formed during the early phases of foreland basin development along the continental margin of Laurentia; the Ordovician examples are related to the Taconian Orogeny whereas the Lower Silurian one is associated with the Salinic Orogeny.

The dolomitization of the Lower and Middle Ordovician carbonates on Anticosti platform occurred shortly after the demise of shallow marine carbonate sedimentation in early Late Ordovician, at a time of significant increase of subsidence rates and associated higher geothermal gradients along the entire continental margin of Laurentia. Two geochemically different fluids are documented; the differences could be related to more pronounced rock-water interactions for the Lower Ordovician carbonates. The dolomitization of the Lower Silurian carbonates on Gaspé Peninsula is demonstrated to be an early event, pre-Late Silurian, which occurred during a significant magmatic period and likely high geothermal gradients. The Lower Silurian hydrothermal dolomites record significant exchanges between the high temperature fluid and the mafic to ultramafic basement that supplied large volumes of Mg^{+2} needed for this regional alteration.

This paper illustrates the tectonic link between active foreland basin and hydrothermal dolomite. Moreover, the efficiency of fault-controlled circulation related to upward thermal convection of dolomitizing fluids is possibly enhanced at times of significant magmatic and thermal episodes along the continental convergent margins.

RÉSUMÉ

Les dolomies dans les successions de l'Ordovicien inférieur et médian d'Anticosti et du Silurien inférieur de la Gaspésie sont démontrées pétrographiquement et géochimiquement comme originant de remplacement précoce et de remplissage ultérieur de cavités à partir de fluides salins de haute température. Ces intervalles riches en dolomites sont interprétés comme des dolomies hydrothermales qui se sont formées lors des phases précoces des épisodes de bassin d'avant-pays sur la marge continentale de Laurentia; les cas de l'Ordovicien étant reliés à l'Orogénie Taconienne et le cas Silurien inférieur est associé à l'Orogénie Salinique.

La dolomitisation des carbonates ordoviciens inférieur et médian de la plate-forme d'Anticosti s'est produite peu de temps après la fin de la sédimentation carbonatée au début de l'Ordovicien tardif, lors d'une période d'augmentation significative des taux de subsidence et des gradients géothermiques associés et ce tout le long de l'ancienne marge continentale de Laurentia. Deux fluides géochimiquement distincts sont documentés, les différences sont associées à des interactions roche-eau plus prononcées pour les dolomies de l'Ordovicien inférieur. La dolomitisation des carbonates du Silurien inférieur de la péninsule gaspésienne est démontrée comme un événement précoce, pré-Silurien supérieur, qui s'est produit durant une période d'importantes activités magmatiques et de gradients géothermiques possiblement élevés. Les dolomies hydrothermales du Silurien inférieur ont enregistré des échanges significatifs entre les fluides de haute température et le sous-bassement mafique et ultramafique, source des grands volumes de Mg^{+2} nécessaires pour cette altération régionale.

Ce papier documente encore plus le lien tectonique entre les bassins d'avant-pays actifs et les dolomies hydrothermales, de plus l'efficacité de la circulation de fluides de dolomitisation le long de failles par convection thermique est possiblement accrue lors d'épisodes magmatiques d'importance le long des marges continentales convergentes.

Introduction

A large number of world-class hydrocarbon reservoirs are hosted by hydrothermal dolomites (HTD) of all ages (Davies and Smith, 2006). Given the economic importance of dolomite reservoirs and the need for improved exploration models, debates are ongoing between workers who are persuaded by the fault-controlled hydrothermal dolomitization process as presented in the summary paper by Davies and Smith (2006) and those who question this model. Timing of dolomitization, nature and origin of the fluid(s), the source of Mg^{+2} for the large volume of dolomite, the ambient conditions during dolomitization and the driving mechanism for fluid circulation still are controversial topics (Machel and Lonnee, 2002; Lonnee and Machel, 2006; Davies and Smith, 2006). Most workers who accept the hydrothermal dolomitization model of Davies and Smith (2006) agree that dolomitization is linked with early (i.e. shortly after inception of burial) episodic, transtensional to extensional faulting and most commonly is associated with the foreland basin stage of a shallow continental margin. This is based on the distribution of dolomite bodies as interpreted from field and core studies and from interpretation of seismic data. However, the regionally higher geothermal gradient associated with increased subsidence rates and magmatic events at the leading edge of the convergent margin is commonly overlooked as a possible critical element for enhancing or even forcing circulation of the high temperature fluids recorded by the hydrothermal dolomite.

In the last few years, a significant number of Paleozoic interpreted hydrothermal dolomites in eastern Canada have been reported (Cooper et al., 2001; Lavoie and Chi, 2001; Chi et al., 2001; Lavoie and Morin, 2004; Lavoie et al., 2005; Lavoie, 2006; Lavoie and Chi, 2006a, 2006b; Knight et al., 2007; Molgat, 2007; Azmy et al., 2008, 2009, Conliffe et al., 2009; Lavoie et al., 2009, 2010a). The dolomitization of the limestone is interpreted to be fault-controlled and, based on petrographic, geochemical and seismic evidence, this event occurred shortly after the onset of burial of the host rock in a foreland basin setting. In eastern Canada, the Lower and Middle Ordovician examples (Anticosti Island) have been related to tectonic activity in the Taconian foreland basin (Lavoie, 1997, 1998; Lavoie et al., 2005, Lavoie and Chi, 2006a), whereas the Lower Silurian examples (Gaspé Peninsula and northern New Brunswick) have been correlated with the initiation of the Salinic foreland basin (Lavoie and Morin, 2004; Lavoie and Chi, 2006b). Other interpreted HTD occurrences in eastern Québec (Lavoie et al., 2009) include the Lower Devonian example (West Point Formation; Lavoie et al., 2010a), which has been linked with the Salinic foreland basin (Lavoie, 2006), and the Lower Devonian example (Upper Gaspé Limestones), which has been correlated with the Acadian foreland basin (Lavoie, 2006).

In this contribution, the spatial and temporal links between hydrothermal alteration of the carbonate successions and major tectono-thermal events are presented for the Paleozoic successions of eastern Québec. The paper will focus on the best known HTD examples that are hosted by the Lower and Middle Ordovician and Lower Silurian rocks (Lavoie and Chi, 2001; Lavoie and Morin, 2004; Lavoie et al., 2005; Lavoie and Chi, 2006a, 2006b; Lavoie et al., 2009). For these examples, a description of the continental margin setting is presented as well as new petrographic and geochemical data for both the Middle Ordovician and Lower Silurian examples. Based on tectono-thermal analysis and on geochemical attributes of the hydrothermal dolomite (published and herein presented), we argue that the fault-controlled upward migration of huge volumes of dolomitizing fluids was enhanced by the regional elevated geothermal gradients associated with the tectonically- and magmatically-active continental margin of Laurentia.

Geological Setting

The successions considered in this contribution occur in two distinct geological domains of eastern Canada: 1) the St. Lawrence Platform (*sensu* Sanford, 1993); and 2) the Gaspé Belt (*sensu* Bourque et al., 1995, 2001).

The St. Lawrence platform

In eastern Canada, the area covered by the St. Lawrence Platform stretches from southern Québec to western Newfoundland (Fig. 1). The preserved succession consists of Cambrian to lowermost Silurian sediments (Fig. 1) that were deposited along the shallow continental shelf of Laurentia after the Late Proterozoic break-up of Rodinia. These mixed siliciclastic-carbonate deposits record the evolution of the margin, from a) the initial rift (latest Proterozoic to Early Cambrian) to b) a passive margin (from Early Cambrian to Early Ordovician) that evolved into c) a tectonically active foreland basin related to the docking of oceanic and/or island arc domains against the Laurentian margin (Middle to Late Ordovician) with the preserved stratigraphic record that ended in d) a successor basin (Late Ordovician to Early Silurian) after the main Taconian accretion event (Sanford, 1993; Lavoie, 2008).

The St. Lawrence Platform succession preserved on Anticosti Island (Figs. 1 and 2) consists of carbonate-dominated facies of Early Ordovician (Arenigian) to Early Silurian (Llandoverian) age. The description here will be limited to the Lower and Middle Ordovician carbonates; readers interested in the overlying succession are referred to Long (2007). The basal unit of the succession is the Lower Ordovician (Arenigian) Romaine Formation, which unconformably overlies Grenvillian metamorphic basement. It consists of eustatically controlled subtidal to peritidal, third- to fifth-order shallowing-upward cycles deposited in a passive-margin setting. The end of Romaine Formation sedimentation was followed by subaerial exposure correlated with the regional Sauk-Tippecanoe sequence-bounding unconformity (Desrochers, 1985; Desrochers and James, 1988; Desrochers et al., in press). Along the continental margin of Laurentia, the development of this unconformity was enhanced by the transit of a

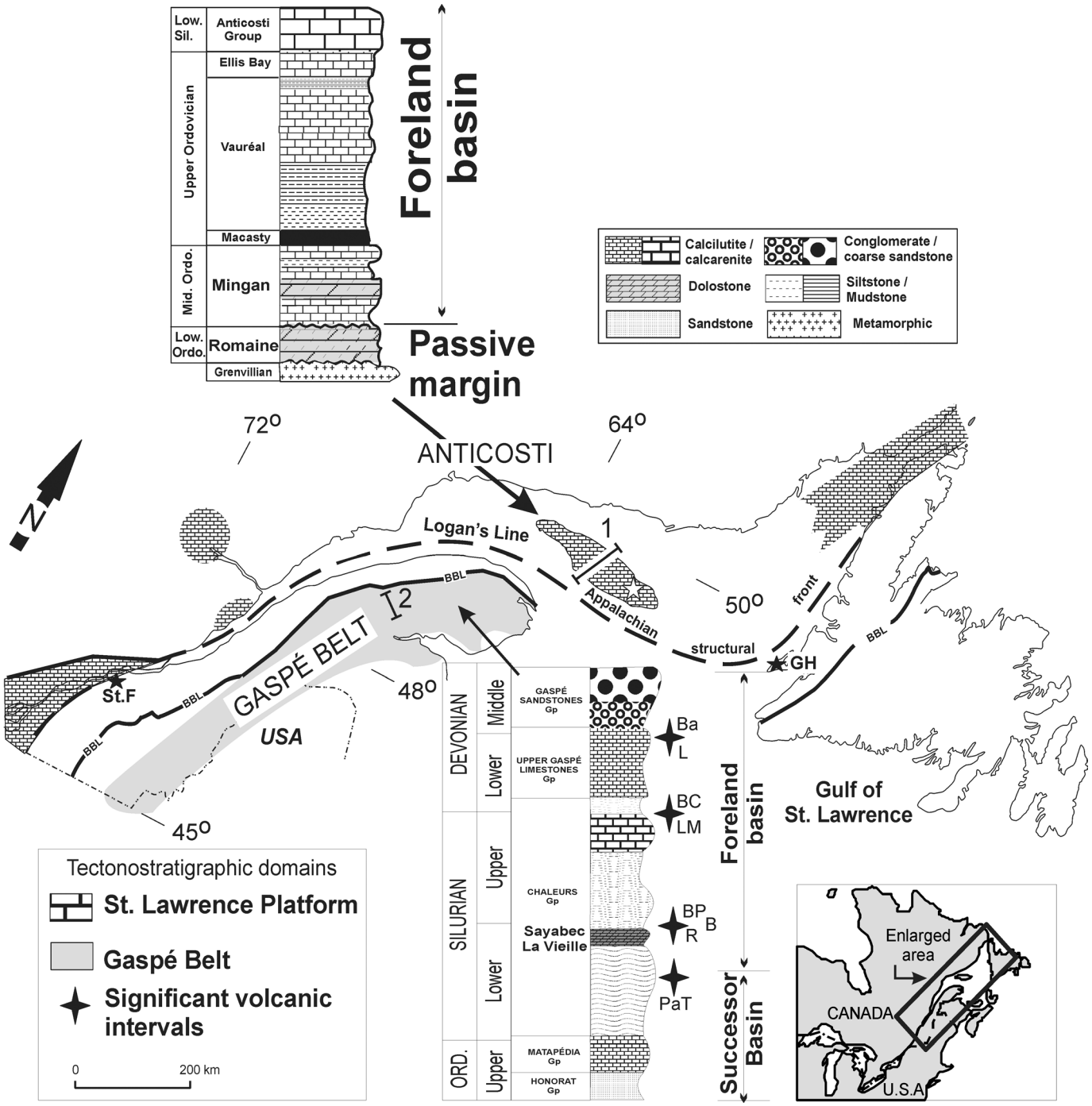

Fig. 1. Simplified geological map of eastern Canada showing the location of the St. Lawrence Platform and the Gaspé Belt and with general representative stratigraphic successions for the Anticosti Island and Gaspé Peninsula. The Romaine and Mingan formations (Ordovician Anticosti) and Sayabec and La Vieille formations (Silurian Gaspé) are positioned in the stratigraphy as well as the significant volcanic units, which include: the Pointe aux Trembles (PaT), Restigouche (R), Benjamin (B), Bryan Point (BP), Lac Mckay (LM), Black Cape (BC), Lyall (L) and Baldwin (Ba). BBL is for Baie Verte – Brompton line; St.F and GH locate the Saint-Flavien gas field and Garden Hill oil field in Lower Ordovician dolomites in southern Québec and western Newfoundland, respectively. Cross-sections 1 and 2 are illustrated on Figures 2 and 3, respectively. White star on Anticosti is the location of seismic line A71-203e shown in Figure 2. Geological map modified from Lavoie et al. (2003). Vertical sections not to scale.

tectonic peripheral bulge on the margin (Jacobi, 1981; Knight et al., 1991). Important lateral thickness and facies changes are present within the upper part of the Romaine Formation and can be linked with foreland basin faulting (Fig. 2; Lavoie, 1997, 1998; Lynch, 2000; Lavoie et al., 2005; Bordet et al., 2006; Desrochers et al., in press). Increasingly more evidence has been gathered in favour of foreland basin onset before the Sauk-Tippecanoe break in eastern Canada (Salad Hersi and

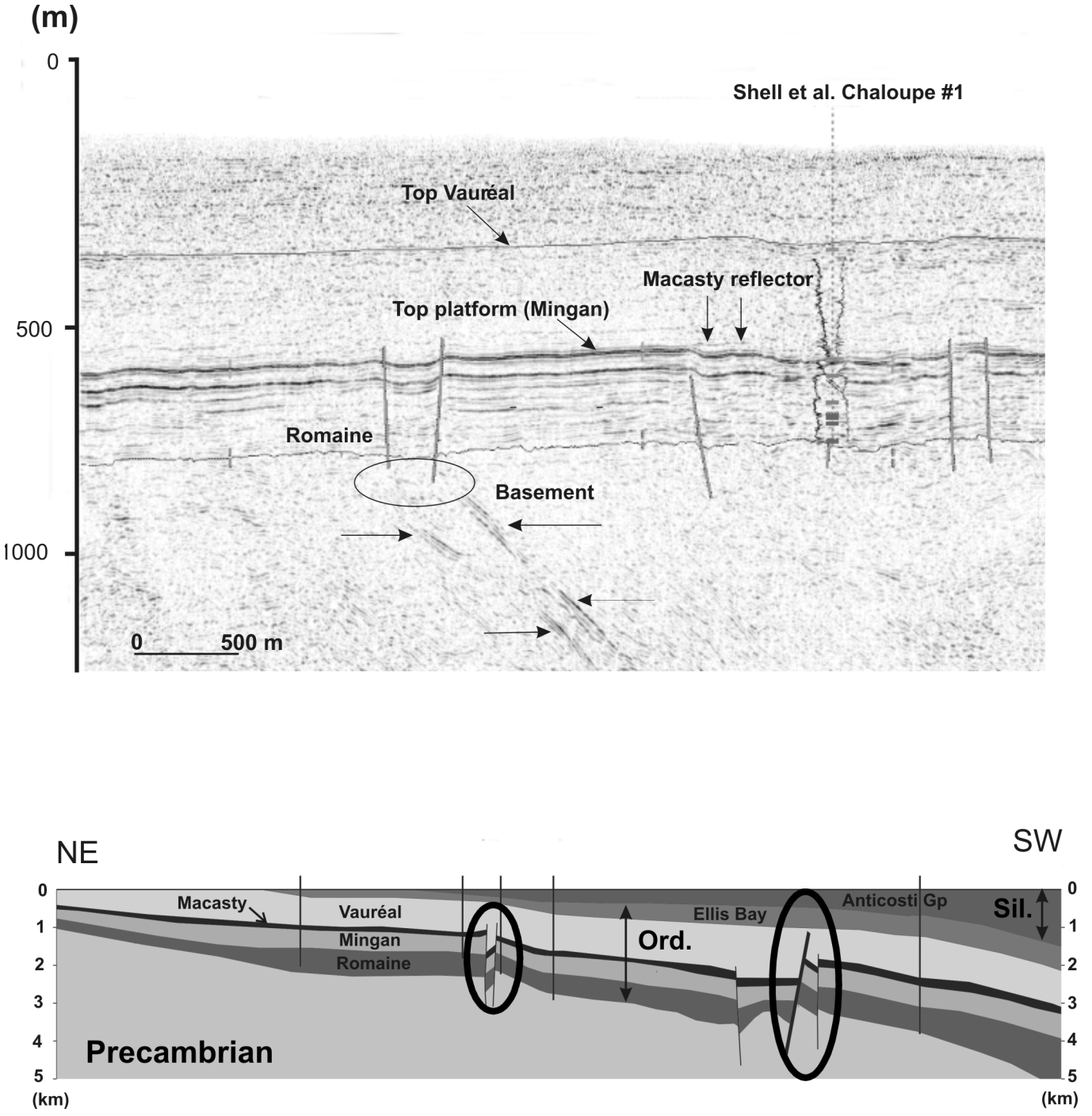

Fig. 2. Top: Part of seismic line A71-203e in eastern Anticosti (white star of Fig. 1) that is tied to the Shell et al. Chaloupe #1 well (Lynch, 2000). Significant reflectors are identified. Some of the extensional faults that cut through the platform and die out in the Macasty seem connected to old, high-angle faults in the Precambrian basement (arrows). The Chaloupe well was drilled in the centre of a sag delimited by extensional faults. The Macasty flat lying reflector overlies the sag. This suggests that the collapse occurred before sedimentation of the Macasty shales. Bottom: Cross-section 1 on Figure 1; the gently southwest-dipping Anticosti platform consists of Lower Ordovician to Lower Silurian facies. This sketch is based on extensive seismic data and some well information. Extensional faults are documented to affect only the Ordovician succession and largely do not extend into the Silurian section. Modified from Castonguay et al. (2005).

Dix, 2006; Dix and Al Rodhan, 2006; Knight et al., 2007; Salad Hersi et al., 2007; Lavoie et al., in press a).

The overlying succession was deposited in an active Taconian foreland basin (Desrochers, 1985; Lavoie, 1994) with a significant increase in subsidence (Long, 2007). The sequence-bounding unconformity is overlain by the Middle Ordovician (Darriwilian-lower Caradocian) Mingan Formation (*sensu* Desrochers, 1985) which consists of a basal transgressive sandstone unit overlain by various peritidal to open marine subtidal carbonate facies. The Mingan Formation recorded a tectonically-controlled sea level rise which eventually led to drowning of the carbonate ramp at the end of the Middle Ordovician (Desrochers, 1985). The Mingan Formation is overlain by the Upper Ordovician Macasty Shale, which recorded the highest subsidence rate in the Anticosti basin (Long, 2007; Chi et al., in press).

From recent seismic and drill hole information, the succession can be described as a gently southwesterly-dipping homocline (Fig. 2) affected by several normal faults. Seismic interpretations indicate that these faults affect only the lower part of the succession (pre-Upper Ordovician) and do not reach the surface (Fig. 2; Lynch, 2000; Bordet et al., 2006, this issue).

Based on organic matter reflectance data and basin modelling (Bertrand, 1987, 1990), the burial of the Romaine Formation to the east of the major extensional Jupiter fault (Lynch, 2000; Lynch and Grist, 2002; Lavoie et al., 2005) reached a maximum of 4.4 km. Thermal modelling suggests that the maximum burial temperatures at the base of the succession have not exceeded 115º–125°C for that part of the island (Bertrand, 1990; Chi et al., in press).

The Gaspé Belt

The Gaspé Belt extends from Gaspé Peninsula to New Brunswick, Maine and southern Québec (Figs. 1 and 3). The succession preserved in the Gaspé Belt consists of Upper Ordovician to Middle Devonian rocks (Fig. 3) that were deposited after the Taconian Orogeny (Lavoie, 2008). The succession is dominated by siliciclastic and volcanic rocks with facies-distinctive carbonate intervals (Bourque et al., 2001). Significant tectonic activity resumed near the end of the Early Silurian (Bourque et al., 2001; Lavoie and Morin, 2004; Lavoie, 2008) with the docking of terranes of Pan-African affinity (the leading Ganderia and trailing Avalonia microcontinents; van Staal, 2005). The Silurian accretion through NW-oriented subduction of Ganderia (Salinic Orogeny) and the continued oblique (strike-slip) convergence of Avalonia until its accretion near the end of the Early Devonian resulted in a long lasting foreland basin history for the Gaspé Belt in eastern Québec (Kirkwood et al., 2004; van Staal, 2005; Pinet et al., 2008).

Increasing evidence indicates that the Gaspé Belt was an active foreland basin shortly after the end of the Taconian Orogeny (Kirkwood et al., 2004). Extensional faults were active in Early Silurian (late Llandoverian) and affected the slightly younger Wenlockian carbonate ramp from northern Gaspé to northern New Brunswick (Lavoie et al., 1992; Bourque et al., 2001; Lavoie and Chi, 2006b). Field observations and seismic data in northern Gaspé show that the Shickshock Sud fault, an Acadian (Middle Devonian) dextral strike-slip fault, had an earlier extensional history (Morin and Laliberté, 2002; Sacks et al., 2003; Desaulniers, 2005). Pervasively dolomitized sections of the Lower Silurian carbonates are associated with this fault in northern Gaspé (Lavoie and Chi, 2001; Lavoie and Morin, 2004) and with interpreted early extensional faults in northern New Brunswick (Bertrand and Malo, 2004; Lavoie and Chi, 2006b). Coeval with these Silurian-Devonian tectonic events, a significant volume of volcanic material erupted and is preserved at various localities in the Gaspé Belt at surface (Laurent and Bélanger, 1984; David et al., 1985; Bédard, 1986; Doyon, 1988; Wilson, 1992; Dostal et al., 1993; Bourque et al., 2001; Wilson et al., 2004) and in the subsurface (Pinet et al., 2005, 2008).

The Lower Silurian carbonates (Sayabec and La Vieille formations) represent the oldest shallow water limestones in the Paleozoic succession of the northern segment of the Appalachian orogen (Bourque et al., 1986; Lavoie et al., 1992). Their sedimentation coincided with the end of the first shallowing phase that followed the late Middle Ordovician Taconian Orogeny (Bourque et al., 2001; Bourque, 2001). The Lower Silurian carbonates formed a gently south-dipping ramp and consisted of four parallel depositional belts (Lavoie et al., 1992). These are, from nearshore to offshore: 1) a wide peritidal mud flat dominated by microbial communities (laminites, stromatolites, thrombolites); 2) a narrow rim of small bioherms built by a consortium of skeletal metazoans (corals, bryozoans, stromatoporoids), skeletal calcareous algae and microbial communities; 3) a well-sorted lime sand belt and; 4) a deeper water nodular mud belt. Significant volumes of Lower Silurian (Llandoverian to Wenlockian) mafic volcanic units are largely coeval with the construction of the carbonate ramp. These are found in northern New Brunswick (Wilson et al., 2004; Pinet et al., 2005, 2008), southern Gaspé Peninsula (Bourque et al., 2001; Pinet et al., 2005, 2008) and in the Témiscouata (David et al., 1985) regions.

The southern limb of the Lac Matapédia syncline, the area from where Sayabec Formation samples originate (Fig. 3), is in the oil window (Ro between 1.0 and 1.3%; Roy, 2004, 2008) and therefore, never experienced burial temperatures in excess of roughly 150°C. The samples of the La Vieille Formation in northern New Brunswick (Lavoie and Chi, 2006b) are from sections characterized by significantly higher thermal maturation with Ro values of the dry gas zone (between 1.8 and 2.2%, Bertrand and Malo, 2004) and, therefore, have likely experienced higher maximum temperatures.

Methods

The values reported herein for fluid inclusions microthermometric data as well as oxygen and carbon isotopic ratios come from Lavoie and Chi (2001; Sayabec Formation), Lavoie and Morin (2004; Sayabec Formation), Lavoie et al. (2005;

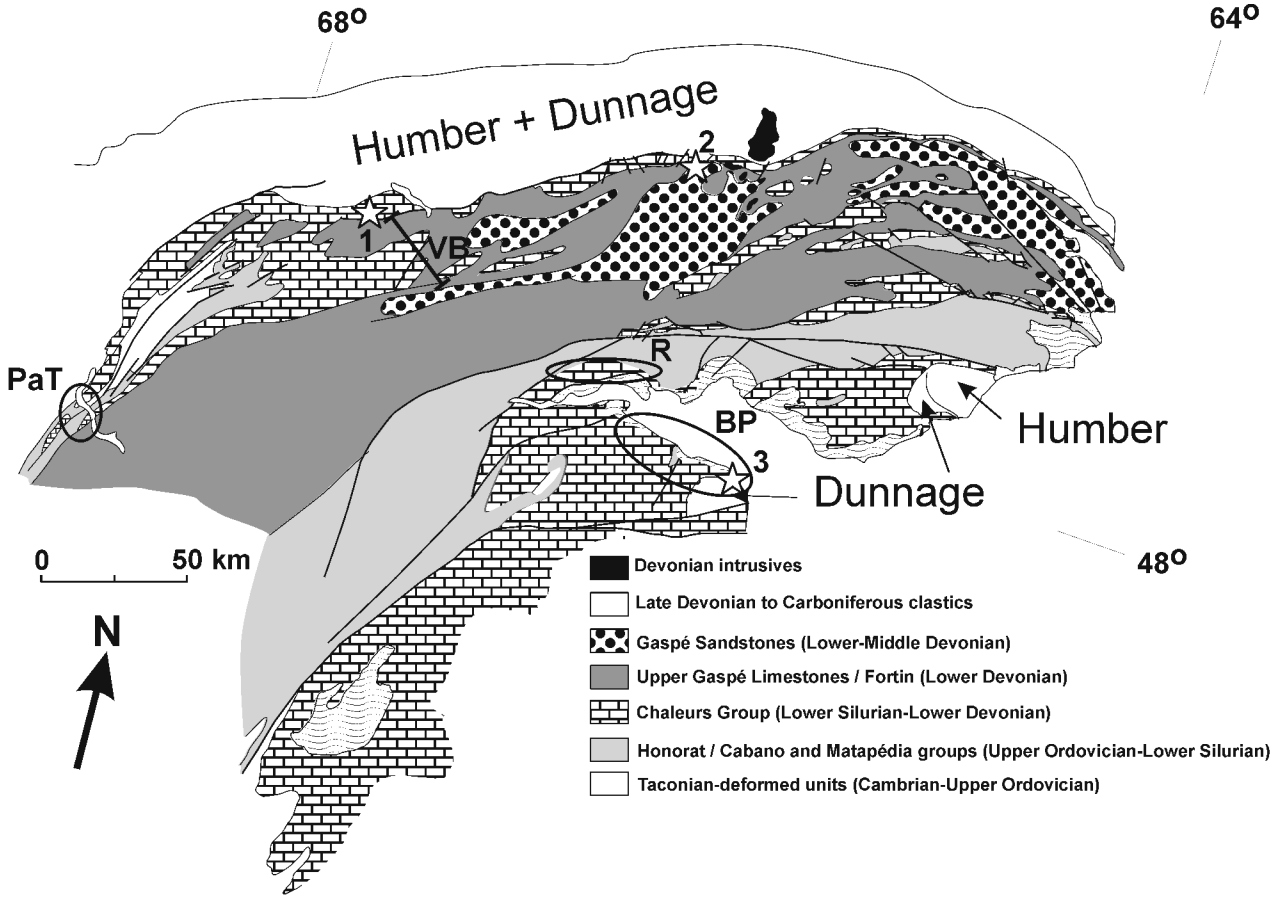

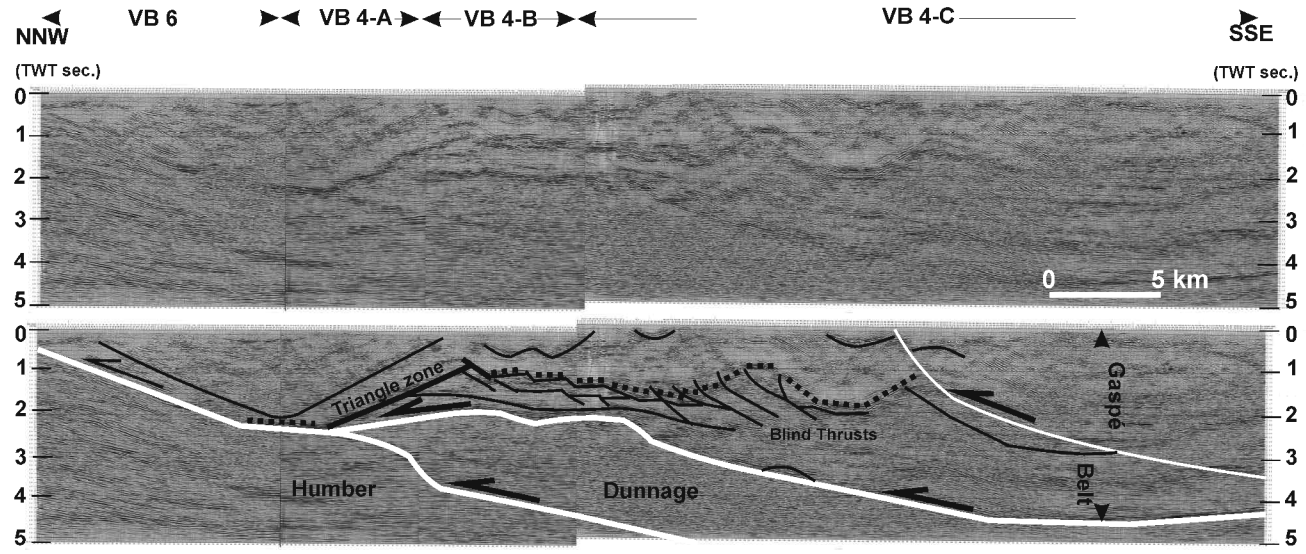

Fig. 3. Geological map of the Acadian Gaspé belt, at the group level (Modified from Bourque et al., 2001). The stars locate the position of three areas with significant hydrothermal dolomites in the Lower Silurian carbonates. 1) Lac Matapédia Syncline, 2) the Ruisseau Isabelle section and 3) the Elmtree Inlier area. VB locates the seismic line shown at the bottom. Ellipses locate areas with significant Llandoverian-Wenlockian volcanic units; PaT is for Pointe aux Trembles Formation (Llandoverian; David and Gariepy, 1990), R is for Restigouche volcanics (Wenlockian?) and BP is for Bryan Point Formation (Wenlockian; Walker et al., 1993). Bottom: the VB seismic line is a composite of 4 lines that illustrate the general tectonic style for the Acadian Gaspé Belt. The Lower Silurian succession is involved in duplexes and other compressive deformation features in the subsurface. The dashed line is the interpreted top reflector of the Sayabec-La Vieille formations seismostratigraphic interval. Modified from Morin and Laliberté (2002).

Romaine Formation) and Lavoie and Chi (2006b; La Vieille Formation). The acquisition of new data for fluid inclusions and stable isotopic ratios for the Mingan (samples from the Shell et al. Chaloupe well, Figs. 1 and 2) and Sayabec (samples form the Lac Matapédia syncline; Fig. 3) formations follow the same analytical procedures presented in those papers. The new carbon ($\delta^{13}C_{PDB}$) and oxygen ($\delta^{18}O_{PDB}$) stable isotopes analyses were performed at the Delta Lab of GSC-Québec with a data precision better than ± 0.1‰. This contribution also reports some new $^{87}Sr/^{86}Sr$ ratios and concentrations of Sr for the Romaine and Mingan formations. The samples for strontium analyses come from wells identified in Lavoie et al. (2005); the analyses were carried out at the AURIF laboratory at Memorial University of Newfoundland. The $^{87}Sr/^{86}Sr$ precision is better than 0.000037 with an accuracy better than 0.000068. The NBS 987 standard reference material was used for calibration of the measured $^{87}Sr/^{86}Sr$ ratios and its average value was 0.710250 ± 0.000028 based on 6 measurements.

Hydrothermal Dolomites in Ordovician Foreland Basins

In eastern North America, Middle to Upper Ordovician HTD are oil and gas reservoir rocks in the Michigan (Hurley and Budros, 1990) and in the Appalachian (Smith, 2006) basins and in southern Ontario (Carter et al., 1996; Molgat, 2007). Oil production from the Lower Ordovician strata in western Newfoundland (Garden Hill field; Cooper et al., 2001) has been documented and historical production of natural gas from Lower Ordovician in southern Québec is known (Saint-Flavien field; Bertrand et al., 2003) (Fig. 1). Lower and Middle Ordovician HTD occurrences, with locally significant amounts of hydrocarbon, have been documented in the St. Lawrence platform of Anticosti Island (Chi et al., 2001; Lavoie et al., 2005, 2009; Lavoie and Chi, 2006a; Chi et al, in press) and southern Québec (Chi et al., 2000; Lavoie et al, 2009) as well as in the Lower Ordovician of New York (Slater et al., 2007). Therefore, from western Newfoundland to the Appalachian Basin in eastern USA, hydrothermal alteration of Lower to Upper Ordovician successions has generated significant fault-controlled, regional masses of dolomites.

Lower Ordovician Romaine Formation, Anticosti Island

Petrographic and geochemical data from the Romaine Formation that support hydrothermal dolomitization have been reported in Lavoie et al. (2005). Average microthermometric data [homogenization temperature (T_h) and salinity] for fluid inclusions (FI) in the Romaine Formation are presented in Table 1. The new $^{87}Sr/^{86}Sr$ ratios and Sr concentration values for the dolomite phases in the Romaine Formation are presented in Table 2. Individual dolomite and calcite samples with paired FI T_h and $\delta^{18}O_{PDB}$ data are listed in Table 3.

As discussed in Lavoie et al. (2005), the FI T_h values for a significant number of matrix replacement dolomite RD3 and RD4 as well as those for the pore-filling saddle dolomite (PD1 and PD2) that formed later in the paragenetic succession are higher than the maximum burial temperature (115–125°C) experienced by the Romaine Formation (Fig. 4), especially in the eastern half of the island, arguing for hydrothermal alteration of the rock unit.

Figures 5 and 6 present the interpreted $\delta^{18}O_{SMOW}$ values of the diagenetic fluids responsible for the various dolomite and late (post-dolomite) calcite phases based on their $\delta^{18}O_{PDB}$ ratios and FI T_h values of individual analyses (Table 3). The early replacement dolomite (RD2; Fig. 5) and late pore-filling calcite (PC2; Fig. 6) are both derived from a brine (20.4 to 24.2 and 16 to 31 wt% $NaCl_{equiv}$. for RD2 and PC2, respectively; Lavoie et al., 2005) that originated from an evolved marine precursor as suggested by the $\delta^{18}O_{SMOW}$ ratio of the replacement / precipitating fluid (between –1 to –5‰; Figs. 5 and 6). The later replacement dolomite (RD3) as well as the pore-filling saddle dolomite (PD1 and PD2) record the presence of a heavy isotope-enriched ($\delta^{18}O_{SMOW}$ between +2 to +6‰; Fig. 5) and very saline (17.0 to 26.5 wt% $NaCl_{equiv}$.; Table 1) fluid. All the dolomites (RD2, RD3, PD1 and PD2) of the Romaine Formation are characterized by $^{87}Sr/^{86}Sr$ ratios (0.709142 to 0.712862; Table 2 and Fig. 7) that are higher than those of Early Ordovician marine seawater (0.7087 to 0.7089; Shields et al., 2003; Fig. 7); some of them are in fact more radiogenic than any value for the Phanerozoic oceans. Because no significant siliciclastic unit is present below the Romaine Formation, the high radiogenic isotope ratios suggest that the dolomitizing brines had profound interactions with the underlying Grenvillian basement. The $\delta^{13}C_{PDB}$ ratios of the Romaine Formation dolomites correlate well with the proposed values for the Arenig seawater (–3.0 to +0.3; Shields et al., 2003; Fig. 7), suggesting that Lower Ordovician carbonates sourced the HCO_3^- for dolomite replacement or precipitation. The interpretation derived from the $\delta^{18}O_{SMOW}$ and $^{87}Sr/^{86}Sr$ values of the dolomitization fluids further strengthen the interpretation of Lavoie et al. (2005) that dolomitization of the Romaine Formation proceeded from high temperature brines that significantly interacted with basement units.

Middle Ordovician Mingan Formation, Anticosti Island

The Middle Ordovician Mingan Formation recently became the prime target for the hydrothermal dolomite play in Anticosti Island (Lynch, 2000; Lavoie et al., 2009). The depositional facies of studied samples for the Mingan Formation are represented by subtidal bioclastic and intraclastic wackestone to grainstone, and no peritidal facies were noted (Chi et al., 2001). The available data set (thin sections, FI microthermometric data, oxygen and carbon stable isotopes, strontium isotope ratios and Sr content) is less abundant than for the Romaine Formation.

Table 1. Fluid-inclusion microthermometric data

Sample	Host mineral	Occurrence	$T_{m\text{-}ice}$(°C) Range	$T_{m\text{-}ice}$(°C) Mean (n)	Salinity (wt.% NaCl equiv.) Range	Salinity (wt.% NaCl equiv.) Mean (n)	T_h (°C) Range	T_h (°C) Mean (n)
Mingan Formation (NEW DATA)								
CHA-5	M-RD2	Along edge of cloudy core	-22.2	-22.2 (1)	23.4	23.4 (1)	85.2 to 96.2	90.7 (2)
		Along edge of cloudy core	-22.9	-22.9 (1)	23.6	23.6 (1)	100.4	100.4 (1)
		Along edge of cloudy core	-22.1 to -24.1	-23.1 (2)	23.4 to 23.8	23.6 (2)	82.8 to 93.7	89.1 (3)
CHA-6	M-RD2	Isolated in clean rim	-23.0	-23.0 (1)	23.6	23.6 (1)	106.8	106.8 (1)
		Isolated in clean rim	-24.7	-24.7 (1)	24.0	24.0 (1)	97.5	97.5 (1)
		Isolated in clean rim	-24.9	-24.9 (1)	24.0	24.0 (1)	102.1	102.1 (1)
CHA-4	M-RD3	Isolated in clean rim	-24.5	-24.5 (1)	23.9	23.9 (1)	108.4	108.4 (1)
		Along edge of cloudy core	-20.7 to -22.4	-21.6 (2)	22.8 to 23.5	23.2 (2)	116.2 to 127.5	121.9 (2)
		Along edge of cloudy core	-27.2	-27.2 (1)	24.7	24.7 (1)	112.8	112.8 (1)
		Along edge of cloudy core	-26.2 to -27.4	-26.8 (1)	24.4 to 24.7	24.6 (2)	101.6 to 106.1	103.8 (3)
Romaine Formation (average values from Lavoie et al., 2005)								
	RD2		-25.5 to -17.3		20.4 to 24.2	22.7 (5)	55.6 to 98.2	74.9 (5)
	RD3		-33.4 to -8.3		12.1 to 26.6	22 (65)	59.4 to 138.5	100.1 (116)
	RD4		-19.2 to -14.7		18.4 to 25.5	22.7 (4)	78.3 to 121.5	92.2 (9)
	PD1		-28.9 to -13.6		17.5 to 25.2	22.2 (10)	60.3 to 113.3	93.3 (24)
	PD2		-32.8 to -13.1		17.0 to 26.5	22.5 (32)	92.1 to 151.0	120.2 (61)
Sayabec Formation (average values from Lavoie and Chi, 2001)								
	SD rim		-39.1 to -18.1		21.0 to 28.0	23.4 (14)	148.8 to 194.0	166.8 (22)
	SD core		-25.8 to -20,1		22.4 to 24.3	23.7 (7)	111.1 to 187.5	145.7 (23)
Sayabec Formation (NEW DATA)								
3970	Dolomite	Rim		-21.5 (1)		23.3		178.1 (1)
	euhedral	Rim		-21.0 (1)		23.0		181.1 (1)
		Core		-22.5 (1)		23.5		218.0 (1)
	Calcite	Isolated		-0.0 (1)		0.0		139.2 (1)
	post-dol	Isolated		-0.0 (1)		0.0		144.3 (1)
		Isolated		-0.1 (1)		0.2		178.2 (1)
		Isolated		-0.1 (1)		0.2		145.3 (1)
		Isolated		-0.3 (1)		0.5		Liquid
		Isolated		-0.2 (1)		0.4		Liquid
		Isolated		-0.2 (1)		0.4		Liquid
		Isolated		-0.2 (1)		0.4		Liquid
		Isolated		-0.1 (1)		0.2		Liquid
		Isolated		-0.1 (1)		0.2		Liquid
		Isolated		0.0 (1)		0.0		Liquid
3972	Dolomite	Cloudy core		-		-		164.2 (1)
	(euhedral)	Isolated		-23.9 (1)		23.8		141.6 (1)
		Isolated		-		-		167.5 (1)
	Calcite	Isolated		-0.4 (1)		0.7		123.2 (1)
	(post-dol)	Isolated		-		-		115.0 (1)

Table 2. Oxygen and Carbon isotope ratios and $^{87}Sr/^{86}Sr$ and Sr concentrations for the Mingan and Romaine formations.

Sample	Host Mineral	$\delta^{18}O$‰	$\delta^{13}C$‰	$^{87}Sr/^{86}Sr$	2 Sigma	[Sr] ppm
Mingan Formation						
CHA-5	Calcite early	−5.6	0.5			
CHA-5	M-RD2	−5.4	0	0.708815	0.000011	570
CHA-6	Calcite early	−6.9	0.4			
CHA-6	M-RD2	−4.5	1.7	0.709034	0.000024	613
CHA-4	Calcite early	−6.0	0.1			
CHA-4	M-RD3	−6.0	1.0	0.708838	0.000029	357
Romaine Formation						
NACP-24	RD-2	−5.3	−3.4	0.712862	0.000014	221
LGCP-28	RD-2	−5.5	−0.5	0.709667	0.000011	150
LKA-5	RD-2			0.709907	0.000023	291
CHA-14-1	RD-2	−5.7	−0.3	0.709142	0.000018	109
CHA-14-2	RD-2	−5.8	0	0.709342	0.000018	125
CHA-32	RD-2	−6.3	−2.9	0.709231	0.000024	128
LKA-3	RD-3			0.710208	0.000024	264
NACP-51	RD-3	−5.2	−1.3	0.710002	0.000008	304
LGCP-24	RD-3	−5.9	−0.4	0.709274	0.000026	78
LGCP-25	PD-1	−5.8	−0.2	0.709577	0.000019	93
LGPL-10	PD-2	−8.7	−0.8	0.710594	0.000011	157

Table 3. Paired Th and $\delta^{18}O$ values

Sample	Host mineral	Th (°C)	$\delta^{18}O$‰ (mean)
Mingan Formation			
CHA-5	M-RD2	92	−5.4
CHA-6	M-RD2	102	−4.5
CHA-4	M-RD3	111	−6.0
Romaine Formation			
LGCP-14	RD2	76	−8.3
QFT-1	RD2	75	−6.1
NACP-39	RD3	110	−5.3
NACP-40	RD3	97	−5.9
NACP-44	RD3	101	−5.0
NACP-46	RD3	109	−5.8
NACP-51	RD3	100	−5.2
LGCP-14	RD3	110	−7.6
LGCP-18	RD3	103	−5.8
LGPL-10	RD3	90	−6.4
QFT-1	RD3	91	−7.4
CHA-14	RD3	102	−5.8
CHA-32	RD3	105	−6.3
LGCP-3	PD1	97	−6.4
LGCP-25	PD1	89	−5.8
LGCP-24	PD2	116	−8.5
LGPL-10	PD2	119	−8.7
NACP-44	PC2	88	−10.1
NACP-51	PC2	78	−10.2
LGCP-28	PC2	63	−9.8
LGCP-31	PC2	43	−7.9
Sayabec Formation			
3970	Matrix	192	−7.8
3972	Matrix	158	−7.3

Microthermometric data from fluid inclusions [homogenization temperature (T_h) and salinity] for replacement dolomites are presented in Table 1. The $\delta^{18}O_{PDB}$ and $\delta^{13}C_{PDB}$ ratios as well as the $^{87}Sr/^{86}Sr$ ratios and Sr concentration values are presented in Table 2, while individual dolomite samples with paired FI T_h and $\delta^{18}O_{PDB}$ data are listed in Table 3.

The paragenetic succession, based on limited thin sections from core indicates that early and later replacement dolomites are present in the unit (Figs. 8 and 9). The Mingan Formation is characterized by initial calcite cementation that commonly fills most of available primary pore space. Based on our limited data set, replacement dolomitization was initiated before onset of stylolitization and continued afterwards. The replacement dolomites share petrographic similarities with the Romaine Formation replacement phases, including sub-mm (0.01 to 0.15 mm) crystals of planar-e type (Sibley and Greg, 1987), dull reddish to non-luminescence under CL, and low iron content (Fig. 8 a to d). In some samples, post-stylolite replacement dolomite (M-RD3) fills irregular stringers that cut through the depositional facies (Fig. 8e, f). Locally, sphalerite and barite are observed as the last diagenetic phases postdating late calcite and dolomite cements. Saddle dolomite, either as a replacement phase or as pore-filling cement, was not observed in core thin sections, although examination of thin sections from cuttings allowed identification of some fragments of this specific dolomite.

The calculated salinities of fluid inclusions within replacement dolomites of the Mingan Formation indicate alteration by highly saline brines (22.8 to 24.7 wt% $NaCl_{equiv.}$; Table 1). The FI T_h values of replacement dolomites (83° to 128°C) closely match those of replacement dolomites of the Romaine

Formation (Table 1), suggesting similar thermal conditions for the replacement of the limestone host. This observation further argues for the hydrothermal nature of the dolomitizing fluids, as the Mingan Formation was certainly buried less deeply than the Romaine Formation. The plot of paired FI T_h and $\delta^{18}O_{PDB}$ data (Fig. 5) indicates that the interstitial brines responsible for dolomitization of the Mingan Formation were heavy isotope-enriched fluids ($\delta^{18}O_{SMOW}$ of +4 to +5‰), similar to those responsible for the late replacement and saddle dolomites in the Romaine Formation. The $^{87}Sr/^{86}Sr$ ratios for the replacement dolomites for the Mingan Formation (0.708815 to 0.709034; Table 2) are less radiogenic than the replacement dolomites in the Romaine Formation (Fig. 7), but are more radiogenic than the interpreted Darriwilian seawater (0.7082 to 0.7086; Shields et al., 2003; Fig. 7). Still, the limited available data set could indicate that the fluids were derived from the Arenig seawater (Fig. 7). The $\delta^{13}C_{PDB}$ ratios of the Mingan Formation dolomites plot at the heavy end of the Darriwilian marine values (–2.5‰ to +1.8‰; Shields et al., 2003; Fig. 7) and are enriched in heavy isotopes compared to Arenigian marine values (Fig. 7); this suggests that most of the HCO_3^- for replacement dolomite in the Mingan Formation was recycled from the precursor marine carbonates.

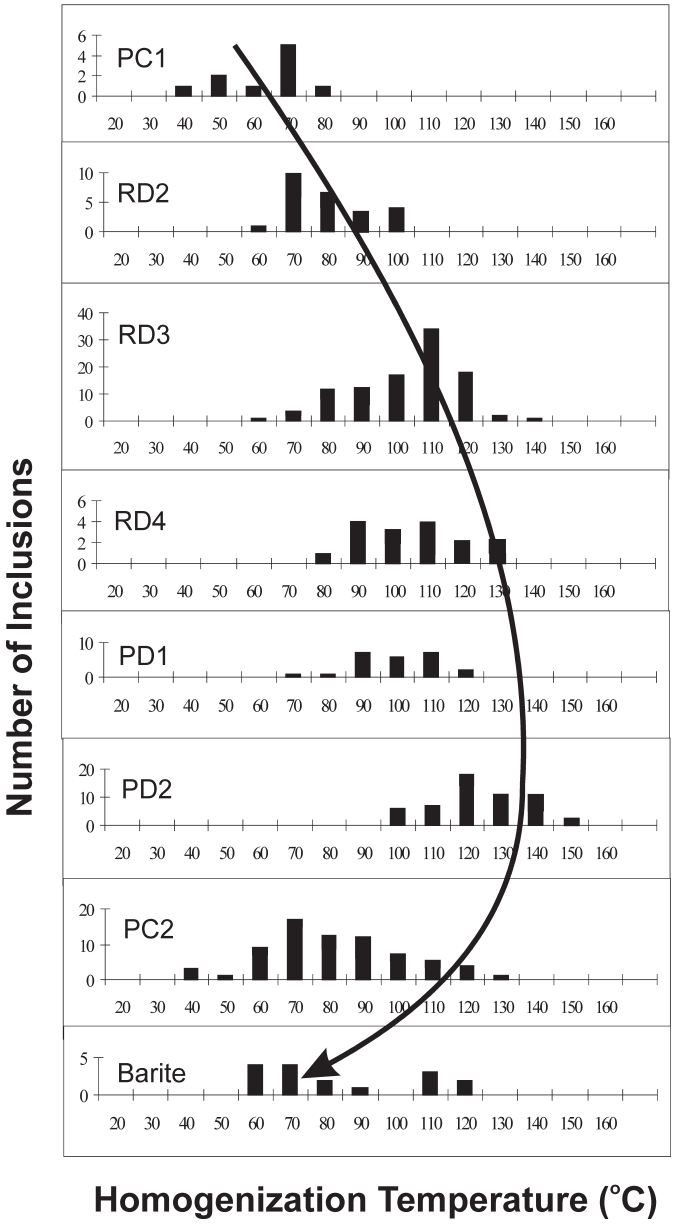

Fig. 4. Summary of paragenetic succession for the Romaine Formation (progressively younger towards the bottom) with FI T_h values. RD is for replacement dolomite, PC and PD are for pore-filling calcite and dolomite, respectively. The arrow outlines the progressive increase in FI T_h values. Modified from Lavoie et al. (2005).

Shallow burial high temperature alteration events in Ordovician carbonates

Dolomitized zones are invariably associated with a well-developed fracture network (Lavoie, 1997, 1998; Lynch, 2000; Chi et al., 2001), and significantly dolomitized intervals in both units

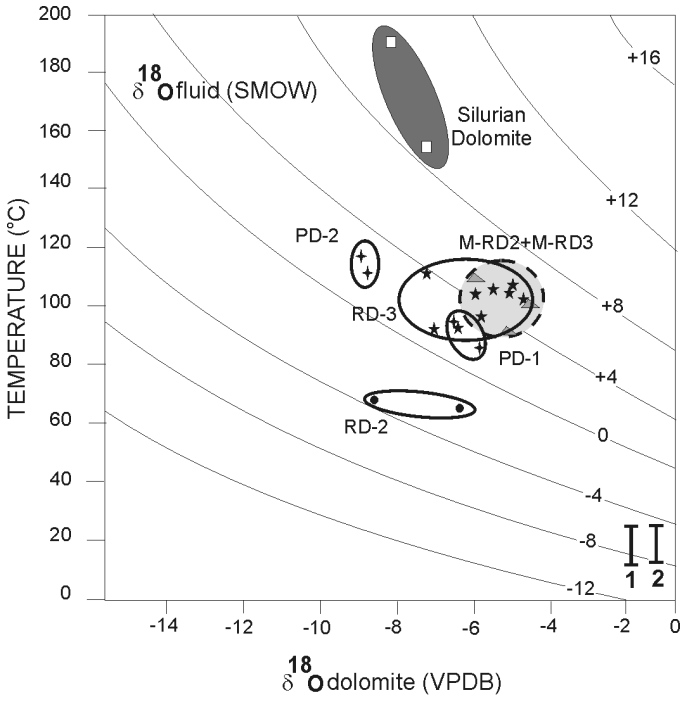

Fig. 5. Temperature (T_h) of fluid inclusions *versus* $\delta^{18}O_{dolomite}$ of specific diagenetic phases. The lines represent $\delta^{18}O_{fluid\text{-}SMOW}$ values that are expected from combined temperatures and oxygen isotopic ratios of dolomites. The equilibrium lines were constructed from the equation $10^3 \ln \alpha = 3.2 \times 10^2 T^{-2} - 3.3$ (Land, 1983). Values for the Romaine Formation are RD-2, RD-3, PD-1 and PD-2 fields, values for the Mingan Formation are M-RD2 and M-RD3 (pale shaded field), finally the values for the Sayabec Formation (Silurian dolomite) are part of the dark-shaded field. The Romaine Formation RD-2 field likely records marine fluid ($\delta^{18}O_{fluid\text{-}SMOW}$ of –4 to –3‰) whereas Romaine Formation RD-3, PD-1 and PD-2 as well as the M-RD2 + M-RD3 field of the Mingan Formation suggest isotopically heavy fluids ($\delta^{18}O_{fluid\text{-}SMOW}$ of +1 to +6‰). Finally, the Silurian values are anomalously enriched in heavy isotopes ($\delta^{18}O_{fluid\text{-}SMOW}$ of +8 to +10‰). Data in Table 3. The bars 1 and 2 (lower right) provide the ranges of assumed sea water $\delta^{18}O_{SMOW}$ composition in 1: Arenig time (–9 to –5.4‰) and 2: Darriwilian time (–8.6 to –5‰) (Shields et al., 2003).

are found in cores drilled in fault-delineated seismic sags (Fig. 2; Lynch, 2000). From core observations and for both the Romaine and Mingan formations, extensional faults and fractures were critical in the circulation of the high temperature saline fluids (Lavoie, 1997, 1998). From seismic data, the sags on top of the Middle Ordovician carbonate succession are filled by the fault-sealing, Upper Ordovician Macasty Shale that immediately overlies the Mingan Formation; the former unit is usually not cut by the faults (Fig. 2; Lynch, 2000; Lavoie et al., 2009). Hence, it can be interpreted that the high temperature, fault-focussed fluid event that resulted in the replacement dolomite in the Mingan Formation occurred early in the burial history of that unit.

Chi et al. (2001) and Lavoie and Chi (2006a) proposed that the significant differences in $^{87}Sr/^{86}Sr$ and Sr concentration values for the replacement dolomites between the Romaine and Mingan formations could be related to two different fluid systems: one that circulated deep into the basement, became

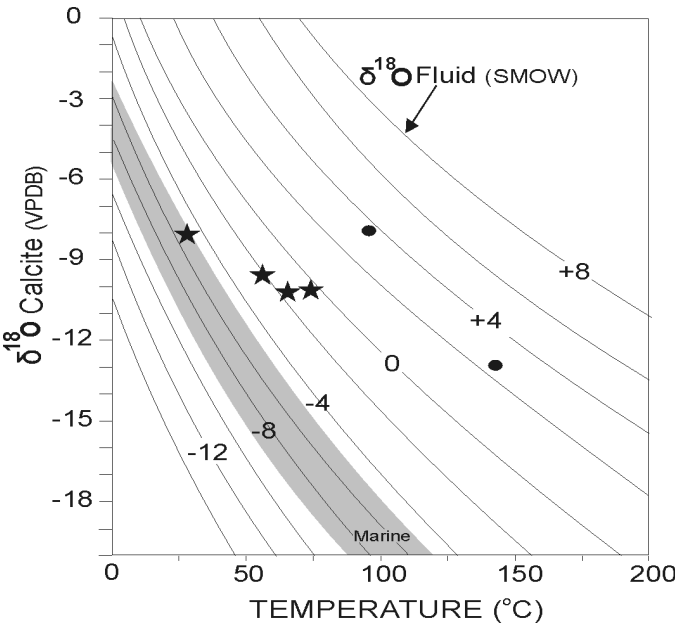

Fig. 6. Temperature (Th) of fluid inclusions *versus* $\delta^{18}O_{calcite}$ composition of late pore filling calcite cement of the Romaine Formation (stars symbols - PC2) and also reported values for La Vieille Formation early, high temperature calcite cements (dots; Lavoie and Chi, 2006b). The lines represent $\delta^{18}O_{fluid\text{-}SMOW}$ values that are expected from combined temperatures and oxygen isotopic ratios of calcites. The equilibrium lines were constructed from equation of Friedman and O'Neil (1977). Values for PC-2 are slightly enriched in heavy isotopes compared to Arenigian sea water (the shaded field; –9 to –5.4‰, Shields et al., 2003). For comparison, the Lower Silurian La Vieille Formation early calcite cement (intimately associated with early dolomite; see Lavoie and Chi, 2006b) is derived from a significantly heavy isotope fluid. Romaine Formation data in Table 3.

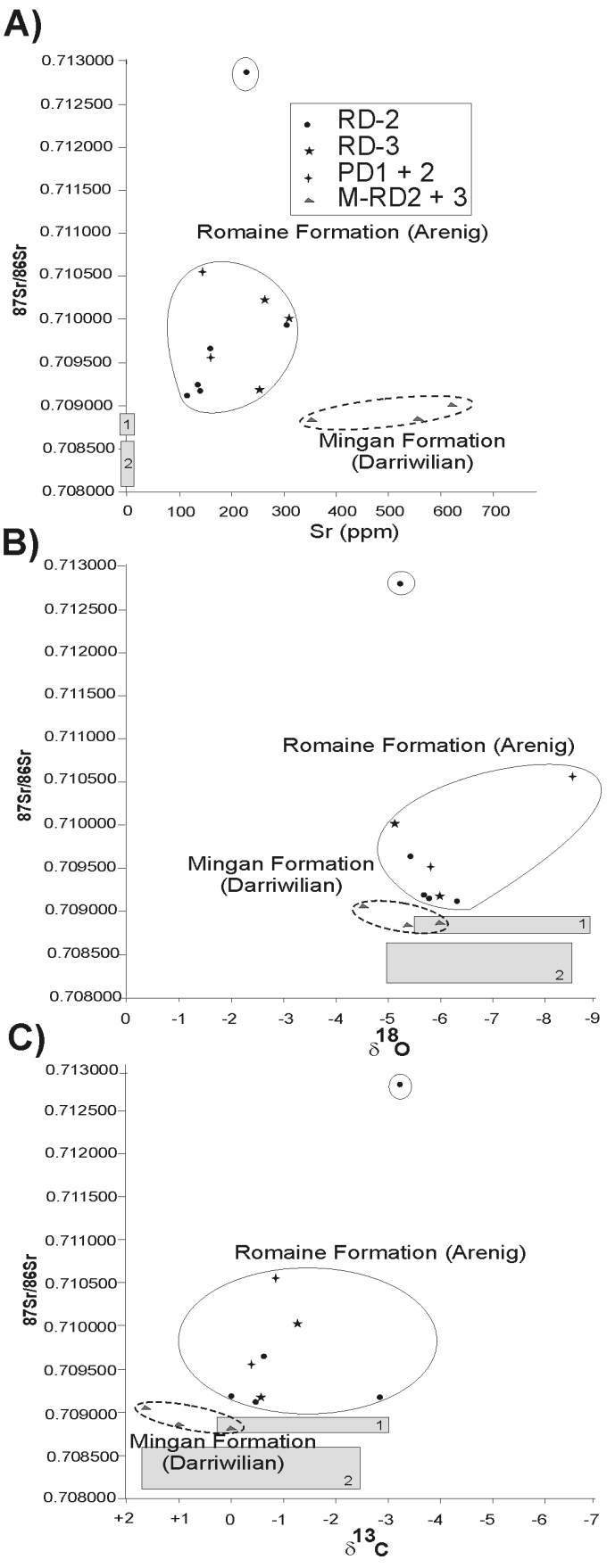

Fig. 7 (right column). Scatter diagram presenting $^{87}Sr/^{86}Sr$ values for the Romaine and Mingan Formations versus A) absolute Sr content in specific dolomites, B) $\delta^{18}O_{PDB}$ of dolomite phases and C) $\delta^{13}C_{PDB}$ of dolomite phases. Data in Table 2. See text for details. For all graphs, the fields for late Arenig and Darriwilian seawater (1 and 2, respectively) are shown by the shaded boxes (Shields et al., 2003).

enriched in ^{87}Sr, and ascended along faults; and another one that moved laterally towards the faults along the strata. Although both fluids may have originated from Arenigian sea water, the former has experienced more fluid-rock interactions than the latter and is consequently enriched in ^{87}Sr and depleted in Sr content. The first fluid dominated in the dolomitization of the Romaine Formation, whereas the second was volumetrically more important in the Mingan Formation.

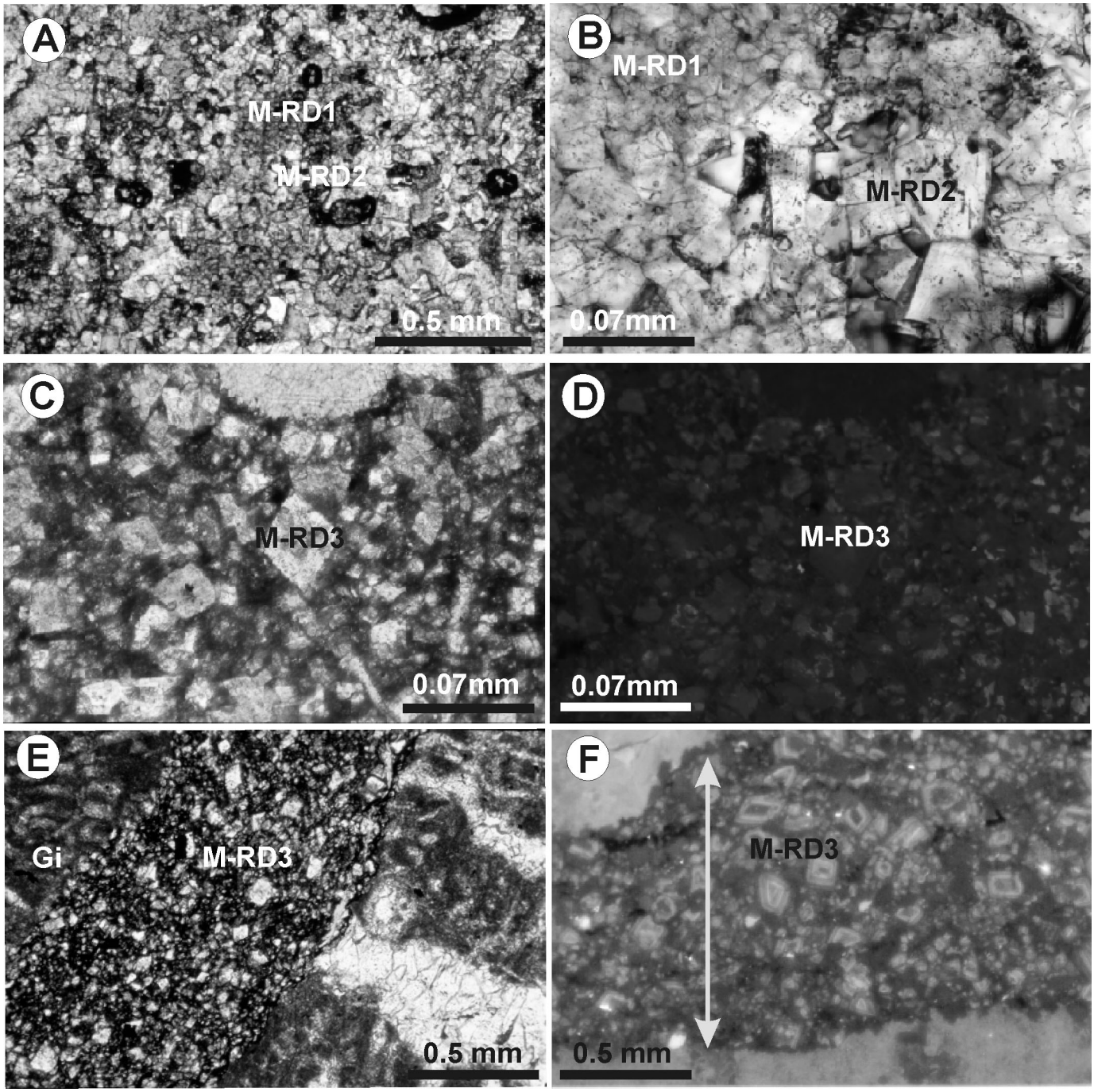

Fig. 8. Dolomites in the Mingan Formation. A) Photomicrograph in transmitted light of early replacement (darker M-RD1) and later replacement (M-RD2) dolomites. Sample CHA-4. B) Close up of A) showing replacement dolomites M-RD1 and M-RD2. C) Photomicrograph in transmitted light of dolomite M-RD3 that replaces a biomicrite matrix. Sample CHA-6. D) Same as C but under cathodoluminescence. Replacement dolomite M-RD3 is very dull luminescent (darker zones) whereas the surrounding matrix is slightly more luminescent. E) Photomicrograph in transmitted light of a "corridor" filled with replacement dolomite M-RD3. The dolomite seam cuts through a fractured (calcite-filled) *Girvanella*-rich (Gi) bioclastic packstone. Sample 4151 NACP well. F) Photomicrograph under cathodoluminescence of a dolomite "corridor" (outlined by arrow) filled by M-RD3 replacement dolomite. The dolomite is luminescent-zoned. Sample 4167 NACP well.

High temperature fluid circulation in Taconian foreland basin

Most eastern North American researchers have selected the major faunal and sedimentologic break in the early Middle Ordovician (Whiterockian) as the expression of the transition from passive margin to foreland basin (James et al., 1989; Read, 1989; Knight et al., 1991; Lavoie, 1994). This major break, which is slightly diachronous westerly (Knight et al., 1991; Salad Hersi et al., 2007; Lavoie et al., in press a) coincides with the migration of a peripheral bulge on the continental margin (Jacobi, 1981) and it correlates with the major Sauk-Tippecanoe unconformity in intracratonic basins (Sloss, 1963).

Increasingly abundant evidence indicates that near the end of the Early Ordovician, before the passage of the peripheral bulge, the continental margin was locally characterized by significant to subtle extensional collapse of the margin as expressed in sudden deepening recorded in the facies architecture and in anomalous thickness variations of units (Lavoie, 1997, 1998; Salad Hersi and Dix, 2006; Dix and Al Rohdan, 2006; Lavoie et al., 2005; Salad Hersi et al., 2007). Therefore, it seems likely that an active tectonic setting was developed at least in the late stages of the deposition of the Romaine Formation, so that the upper part of the formation should be considered a foreland-basin deposit (Lavoie et al., in press a).

The Middle to Upper Ordovician Taconian Orogeny is interpreted to have resulted from the accretion on the continental margin of Laurentia of several discontinuous Ordovician volcanic arcs, along a SE-dipping (present-day coordinates) subduction zone (Pinet and Tremblay, 1995; van Staal, 2005). As the collision of the lithospheric plates proceeded, flexural extension from the subduction resulted in the reactivation of some old (rift-related?) Precambrian faults along the continental margin (Fig. 2) and the formation of new faults in the Lower Paleozoic sedimentary pile (e.g. O'Brien et al., 1999). The spatial link between structures in the Precambrian basement and faults in the Lower Paleozoic succession can be seen on a number of seismic lines on Anticosti (Fig. 2 and Lynch, 2000). Such a relationship is also documented in the Appalachian Basin to the south (Smith, 2006). These extensional faults may have provided the main conduits for high temperature saline fluids that were expelled from deeper in the basin; they could also have served as recharge zones for cooler and younger marine fluids to descend into the basement to be chemically altered and heated and eventually, to ascend.

The upward circulation of the dolomitizing fluids was enhanced by an increase of the geothermal gradient that was associated with the significant increase in subsidence rates that is documented in the Upper Ordovician succession on Anticosti Island (Long, 2007). The conclusions of this rock thickness - time interval analysis is supported by Apatite Fission Track data (Lynch and Grist, 2002) which also indicate rapid burial and significant increase of geothermal gradients in Late Ordovician time followed by a general decrease of both rates in Silurian.

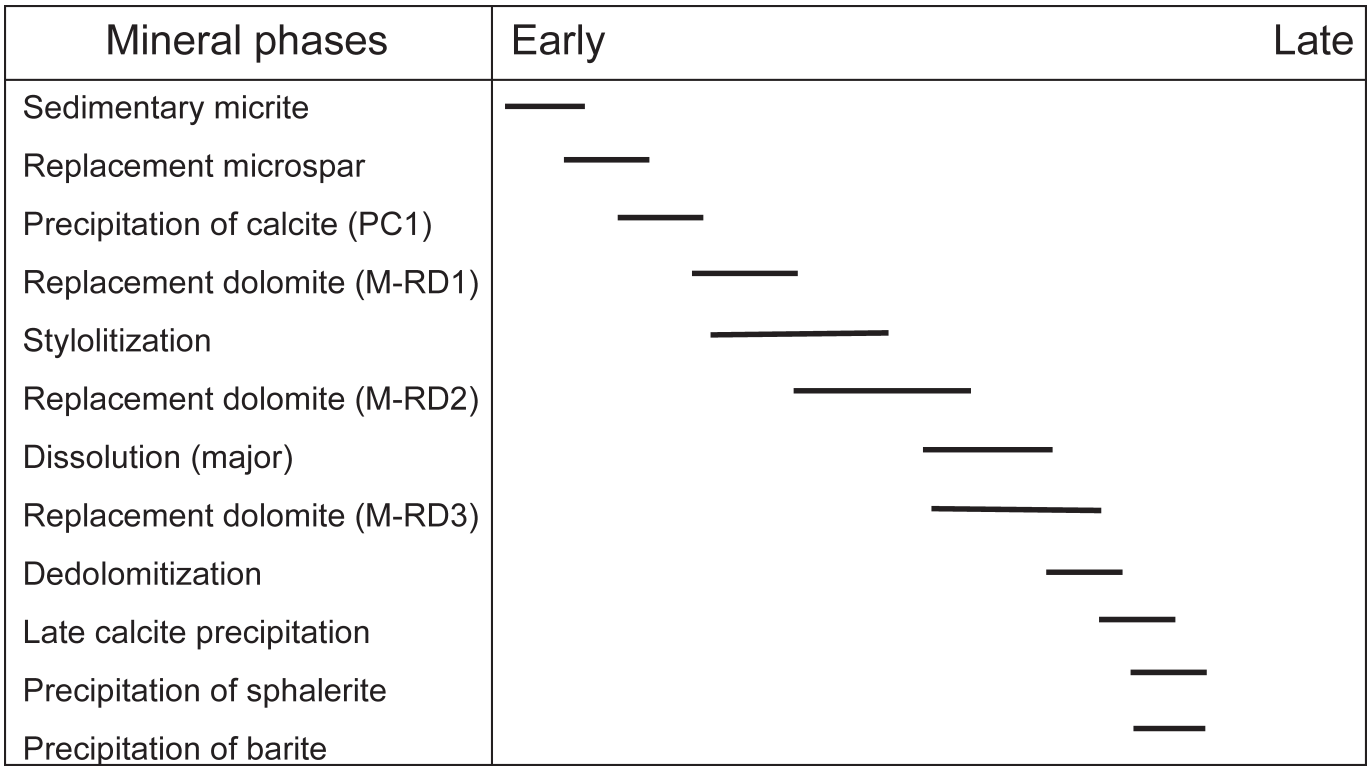

Fig. 9. Summary of the paragenetic succession in the Mingan Formation as recognized from detailed conventional and cathodoluminescence petrography.

Hydrothermal Dolomites in Silurian Foreland Basin

There are few examples of hydrocarbon production from Silurian hydrothermal dolomites in North America; one example is the Silurian Wristen Group in Texas (Davies and Smith, 2006). The outcrop of Lower Silurian HTD in northern Gaspé is characterized by a significant amount of bitumen that fills secondary pore space which makes up to 25–30% of rock volume (Lavoie and Morin, 2004; Lavoie and Chi, 2006b). In the absence of any significant amount of organic matter in those limestone facies (TOC below 0.1%; Bertrand and Malo, 2001, 2004; Roy, 2004, 2008), the pore-filling bitumen cannot realistically be related to forced maturation of organic matter-rich intervals in the succession (Davies and Smith, 2006). The quarry outcrop of the Sayabec Formation on the southern limb of the Lac Matapédia syncline (Fig. 3; Lavoie and Morin, 2004) is interpreted as part of a locally exhumed oil field (Lavoie et al., 2009).

There are no new conventional or cathodoluminescence petrographic data reported here and readers are referred to the cited literature for detailed description of the diagenetic phases for the Gaspé Belt Lower Silurian HTD. Fluid inclusion microthermometric data (T_h and salinity) and $\delta^{18}O_{PDB}$ and $\delta^{13}C_{PDB}$ ratios for diagenetic phases in the Lower Silurian examples are discussed in Lavoie and Chi (2001), Lavoie and Morin (2004) and Lavoie and Chi (2006b). The average FI microthermometric data for the Sayabec Formation saddle dolomite from Lavoie and Chi (2001) are listed in Table 1, which also contains new FI data for dolomite and calcite cements for the Sayabec Formation at the Lac Matapédia syncline (Lavoie and Morin, 2004). Paired FI T_h and $\delta^{18}O_{PDB}$ data from individual analysis are reported in Table 3.

The published and new data for the Lower Silurian dolomites are characterized by very saline fluid inclusions (>21 wt% $NaCl_{equiv.}$; Table 1). The new FI T_h data from dolomites in the Sayabec Formation at the Lac Matapédia syncline (142 to 218°C; Table 1) fall in the same range of high temperatures as those reported from the same unit in central Gaspé (114 to 194°C, Ruisseau Isabelle section; Lavoie and Chi, 2001). These new values are significantly higher than the maximum burial thermal conditions recorded by organic matter in the non-dolomitized limestone facies at that specific section (Ro of 1.3%, ≈ 130° to 150°C; Roy, 2004, 2008). Paired FI T_h and $\delta^{18}O_{PDB}$ values are used to reconstruct the $\delta^{18}O_{SMOW}$ ratio of the fluid responsible for the matrix dolomite (Fig. 4). The data indicate that a very heavy isotope-enriched fluid ($\delta^{18}O_{SMOW}$ of +8 to +10‰) was responsible for the dolomitization. High-temperature calcite cements are found with matrix and saddle dolomite in the La Vieille Formation of New Brunswick, the calcite was documented to have precipitated from a fluid with $\delta^{18}O_{SMOW}$ ratio of +2 to +3‰ (Fig. 5; Lavoie and Chi, 2006b).

The very high $\delta^{18}O_{SMOW}$ ratios of the fluid responsible for the replacement dolomite could suggest either the presence of some exotic fluids or a significant enrichment of marine-derived fluid from pronounced interactions with evaporative-derived brines. Evaporite deposits are currently unknown in eastern Canada in the Paleozoic section until the Carboniferous, well after the early dolomitization of the Lower Silurian carbonates (see below). The Sayabec and La Vieille formations stratigraphically overlie significant Ordovician ultramafic to mafic basements with a few hundreds of meters of predominantly coarse-grained clastic sediments between the basement and the Silurian carbonate platform (Lavoie and Morin, 2004; Lavoie and Chi, 2006b). Basaltic rocks of arc and MORB affinities are characterized by heavy whole-rock $\delta^{18}O_{SMOW}$ ratios (+5 to +10‰; Harmon and Hoefs, 1984). It is proposed that high temperature fluids not only gained their Mg^{+2} charge from these mafic units (Lavoie and Morin, 2004; Lavoie and Chi, 2006b; Lavoie et al., 2010b), but also obtained the anomalous high $\delta^{18}O_{SMOW}$ ratios by significant interactions with the mafic rocks.

Important new FI microthermometric data from late calcite cements from the Sayabec Formation in the Lac Matapédia syncline are reported (Table 1). The fluid inclusions in the host calcite are non-saline and as such, mark a major shift from the earlier dolomite. The calcite cement post-dated both the hydrothermal dolomitization and the significant hydrocarbon charge in the secondary pore space (Lavoie and Morin, 2004). From the strongly-zoned luminescence characteristic of the cement itself, its presence on scalloped or corroded post-dolomite surfaces, and its characteristic narrow range of $\delta^{18}O_{PDB}$ and wide scatter of $\delta^{13}C_{PDB}$ ratios, Lavoie and Morin (2004) provisionally interpreted this calcite as a meteoric calcite cement related to the Late Silurian sub-aerial exposure of part of the Lower Silurian succession (Lavoie and Bourque, 1993). A similar interpretation, based on petrographic and geochemical data, was proposed for late calcite cement in the La Vieille Formation of New Brunswick (Lavoie and Chi, 2006b). For the La Vieille and Sayabec formations (Lavoie and Chi, 2006b and Table 1, respectively), the FI T_h values for this calcite cement are highly erratic (from one-phase liquid inclusions or likely below 50°C up to 178°C). In both examples, calcite-hosting FI are either one-phase liquid or contain an anomalously large bubble that is commonly interpreted to reflect heterogeneous trapping in the meteoric vadose zone (Barker and Halley, 1988) and, consequently, do not yield reliable T_h values.

Shallow burial high temperature alteration events in Silurian carbonates

Active faulting in the early stages of the burial history of a carbonate host is commonly seen as the most critical prerequisite for significant hydrothermal alteration of a limestone unit (Davies and Smith, 2006). The Lower Silurian succession belongs to a folded and faulted belt (Fig. 3) and the subtle expression of sags is not unequivocally recognized even after flattening of the Lower Silurian seismostratigraphic interval (Desaulniers, 2005). However, the easily picked Lower Silurian seismic interval (Fig. 3) is cut by numerous faults defining zones with subtle thickness variations; a significant number of these faults do not pierce through the top of the overlying fine-grained Upper Silurian Saint-Léon Formation (Desaulniers, 2005). The seismic flattening also helps to document thickness

variations of the Upper Silurian and younger units, the thickening being associated with high-angle normal faults (Desaulniers, 2005). Therefore, recent detailed work on seismic data helps to document that significant extensional (transtensional?) faulting occurred at the time of sedimentation of the Lower Silurian carbonates. The onset of extensional collapse in late Early Silurian has also been documented from field thickness variations and facies architecture in the Lower Silurian (Llandoverian) Burnt Jam Brook Formation (Bourque et al., 1995, 2001) and in the slightly younger (Wenlockian) Sayabec Formation (Lavoie, 1988). Hence, active faulting in the Early Silurian depositional basin is documented from various field and seismic data (Lavoie, 2008).

The sub-aerial exposure event after the hydrothermal dolomitization in both northern Gaspé and New Brunswick is an important element to consider for time relationships. The dissolution of carbonates and the precipitation of meteoric calcite cement are associated with local sub-aerial exposure of the Lower Silurian succession. The exposure could be related to: 1) a widely-recognized Late Silurian global sea level lowstand; 2) the Late Silurian Salinic tectonic uplift; or even 3) the combined effect of both events. Whatever the cause, the result (the Salinic unconformity) is visible at several places in the Gaspé Belt (Lavoie and Bourque, 1993; Bourque et al., 2001; Wilson et al., 2004), which suggests that the fault-controlled high temperature dolomitization of the Lower Silurian carbonates occurred prior to the Late Silurian, therefore shortly after onset of burial of the limestone succession and at relatively shallow burial depth.

Magmatic activity and high geothermal gradients in the Salinic-Acadian foreland basin

Early Silurian tectonism in the Gaspé Belt is related to the accretion of the microcontinent Ganderia against Laurentia, through a NW-dipping (present-day coordinates) subduction plane (Wilson et al., 2004; van Staal, 2005). The presence of an Early Silurian subduction zone is documented in central New Brunswick by the presence of the high pressure – low temperature blueschist assemblage with $^{40}Ar/^{39}Ar$ ages ranging between 442 ± 4 and 430 ±4 Ma (Llandoverian; van Staal et al., 1990). The lithospheric response to the subduction of the leading margin of Ganderia (the Tetagouche – Exploits back arc basin of van Staal, 2005) resulted in the onset of extension along reactivated Taconian faults in the Gaspé forearc basin (Pinet et al., 2008).

In the Gaspé Belt, west of the post-Taconian composite margin, there is little evidence of an active tectonic environment from Late Ordovician to the late Early Silurian (Bourque et al., 2001; Kirkwood et al., 2004). The onset of synsedimentary tectonic activity is recorded in the central part of the basin by fault-controlled anomalous thickening of Lower Silurian units (Bourque et al., 1995, 2001).

Coeval and associated with the subduction, melting of the down-going plate occurred and produced Lower Silurian arc mafic volcanic units that are present in the Témiscouata region (Fig. 3; Pointe aux Trembles Formation, David et al., 1985; David and Gariepy, 1990). These Llandoverian andesitic tuffs and breccias were deposited just before the sedimentation of the regional Lower Silurian carbonate ramp facies and argue for higher geothermal gradients at that time. In southern Gaspé Peninsula and in northern New Brunswick, the Lower Silurian carbonate facies are directly overlain by Wenlockian (423 ± 3 Ma; Walker et al., 1993) within-plate volcanic units (Bryan Point and Benjamin formations and Restigouche volcanics). The presence of volcanic units directly below and above the Lower Silurian carbonate facies is proposed as a strong argument for high geothermal gradients at that time. These higher gradients were also likely associated with the regional increase in subsidence rate that followed the onset of the Salinic foreland basin (Bertrand and Malo, 2001; Kirkwood et al., 2004; Desaulniers, 2005).

Discussion

In eastern Canada, Lower to Middle Ordovician and Lower Silurian hydrothermal dolomites are spatially and temporally linked with the onset of foreland basins and associated increase in subsidence rates and geothermal gradients. Moreover, for the Lower Silurian succession, the carbonate platform is intercalated between volcanic units and occurred at a time of widespread plutonism in the Appalachians (Hepburn et al., 1995; van Staal, 2005). It is noteworthy that other reported examples of interpreted hydrothermal dolomites in the Acadian foreland basin succession of Appalachian Orogen in eastern Canada (Lower Devonian West Point Formation and Lower Devonian Upper Gaspé Limestones; Lavoie, 2006; Lavoie et al., 2010a) are spatially and temporally associated with significant volumes of within-plate mafic volcanic – magmatic units found in central and southern Gaspé Peninsula (Bourque et al., 2001, their figures 6 and 7). In these examples, the magmatic activity is associated with asthenospheric upwelling after lithospheric delamination (van Staal and de Roo, 1995; Wilson et al., 2004; Tremblay and Pinet, 2005).

The generation and subsequent rise of magma from the melting of a down-going plate is responsible for significant, regional-scale upward deflection of thermal isograds in the adjacent lithosphere away from the subduction zone itself (e.g. Grevemeyer et al., 2005; Okubo et al., 2005). Similarly, in extensional domains, the upwellings of the asthenosphere will also result in a significant upward deflection of the thermal isograds in the stretched and thinned crust (e.g. Thomson et al., 2005; Behn et al., 2007). The heat flow and resulting geothermal gradient will increase over significant areas along the margin in either compressive or extensional domains.

Convergent continental margins and their associated, fast subsiding foreland basins are characterized by geothermal gradients that are higher than those of old passive margins they commonly succeed (Taylor et al., 1998), a situation observed for the lower Paleozoic succession of eastern North America (Burden and Williams, 1995, 1996). Magmatic processes active at convergent margins further increase regional geothermal gradients. These high gradients can be a critical element in enhancing and even forcing convection of large volumes of

high temperature brines that could eventually form hydrothermal dolomites provided that the other elements of the system are present (e.g. early active faulting that cuts through favourable porous and permeable carbonate host, source of Mg^{+2} and an efficient unbreached seal; Davies and Smith, 2006). From the significant magmatic processes that take place at a convergent margin, limestone successions deposited in fast subsiding foreland basins could be prime targets for hydrothermal dolomitization. Other high temperature settings such as rifted, young and hot crust (e.g. the Jurassic Deep Panuke field; Wierzbicki et al., 2006) or old (post-rift) crust overlain by still hot mantle plume could also be seen as a potential favourable setting for hydrothermal dolomitization. However, the tectonic environment for repetitive fault reactivation might be more problematic, at least for the latter.

The association of hydrothermal dolomites in rapidly subsiding foreland basins with a record of coeval significant magmatic activity is not restricted to the eastern North American region, as similar relationships are documented for (amongst others) the Devonian-Mississippian of western Canada (Davies and Smith, 2006), the Upper Carboniferous of Spain (Gasparrini et al., 2006) and the Triassic of northern Italy (Wilson et al., 1990). It is proposed that higher geothermal gradients associated with the significant magmatic activity from the inception of the active foreland basins was a critical element in enhancing and forcing upward fault-controlled circulation of hydrothermal fluids. Therefore, in the global search for economic accumulations of hydrocarbons, foreland basins with a long lasting history of significant magmatism especially at the time of carbonate accumulation should be considered as prime targets for the large hydrothermal dolomite fields.

Conclusions

Hydrothermal dolomites have been recognized and characterized in the Ordovician and Silurian successions from the St. Lawrence Platform and Gaspé Belt, respectively. For both examples, the pervasive matrix dolomite and pore-filling saddle dolomite cement originated from ^{87}Sr-enriched (Ordovician examples), saline, high temperature fluids. Alteration of the limestone host occurred relatively early in the burial history of these Middle Ordovician and Silurian successions. The migration of hydrothermal alteration fluids into the limestones was facilitated through active repetitive extensional faulting, a common process in foreland basins (Sibson, 1990, 2000). The accretion events in Ordovician (Taconian Orogeny) and Silurian (Salinic Orogeny) resulted in a tectonic environment with favourable conditions for brittle faulting in the associated shallow foreland at the continental margin.

From the Middle to Upper Ordovician, during the deposition of the Mingan Formation carbonates and younger Ordovician units, a SE-oriented (present-day coordinates) subduction zone generated, through melting of the down-going plate, significant explosive felsic magmas expressed in abundant subaerial volcanic ash layers recorded in eastern USA (Kolata et al., 1996). The volcanic material was deposited on a rapidly subsiding foreland platform and was largely coeval with the early hydrothermal alteration of the Middle Ordovician carbonates in Québec (this paper) and in adjacent New York (Smith, 2006) and Ohio (Sagan and Hart, 2006). Similarly, in the late Early Silurian – early Late Silurian, the collision of Ganderia along Laurentia generated extrusive and intrusive intra-plate mafic magmas at the time of early hydrothermal alteration of the Lower Silurian carbonates in the Gaspé Belt. It is noteworthy that Lower Devonian potential hydrothermal dolomites in the Gaspé Belt are also spatially and temporally associated with significant magmatism of the Acadian Orogeny (Lavoie et al., 2009; Lavoie et al., 2010a). Magmatic activity during foreland basin stages should not be consider as a negative-only element in the evaluation of hydrocarbon prospectivity of a sedimentary basin, as it is the relative timing between all the geological events that dictate the eventual potential of these accumulations.

Acknowledgments

This paper benefited from initial review of N. Pinet and from the detailed and critical reviews of V. Vandeginste, M. Coniglio and K. Osadetz and the appreciated editorial comments of R. MacNaughton. The first author acknowledges the financial contribution of Shell Canada and Corridor Resources for supporting this research on hydrothermal dolomites on Anticosti Island. The data from Anticosti and Gaspé was also generated during the Geological Survey of Canada "Lower Paleozoic forelands and platform" project under the National Mapping program as well as during the "Appalachian Energy" project part of the second phase of the Targeted Geoscience Program. The second author acknowledges continuous support of the Natural Sciences and Engineering Research Council of Canada. This is Geological Survey of Canada contribution 20070106.

References

Azmy, K., Lavoie, D., Knight, I. and Chi, G. 2008. Dolomitization of the Aguathuna Formation carbonates of Port au Port Peninsula in western Newfoundland, Canada: implications for a hydrocarbon reservoir. Canadian Journal of Earth Sciences, v. 45, p. 795–813.

_____, Knight, I., Lavoie, D. and Chi, G. 2009. Origin of dolomites in the Boat Harbour Formation, St. George Group, in western Newfoundland, Canada: implications for porosity development. Bulletin of Canadian Petroleum Geology, v. 57, p. 81–104.

Barker C.E. and Halley, R.B. 1988. Fluid inclusions in vadose cement with consistent vapor to liquid ratios, Pleistocene Miami Limestone, southeastern Florida. Geochimica et Cosmochimica Acta, v. 52, p. 1019–1025.

Bédard, J.H. 1986. Pre-Acadian magmatic suites of the southeastern Gaspé Peninsula. Geological Society of America Bulletin, v. 97, p. 1177–1191.

Behn, M.D., Boettcher, M.S. and Hirth, G. 2007. Thermal structure of oceanic transform fault. Geology, v. 35, p. 307–310.

Bertrand, R. 1987. Maturation thermique et potentiel pétroligène des séries post-taconiennes du nord-est de la Gaspésie et de l'île d'Anticosti. Doctorate thesis, Université de Neufchâtel, Suisse, 647 p., http://www.unine.ch/ biblio.

_____1990. Maturation thermique et histoire de l'enfouissement et de la génération des hydrocarbures du bassin de l'archipel de Mingan et de l'Île d'Anticosti. Canadian Journal of Earth Sciences, v. 27, p. 731–741.

_____ and Malo, M. 2001. Source rock analysis, thermal maturation and hydrocarbon generation in the Silurian-Devonian rocks of the Gaspé Belt basin, Canada. Bulletin of Canadian Petroleum Geology, v. 49, p. 238–261.

_____ and _____ 2004. Maturation thermique, potentiel roche mère des roches ordoviciennes à dévoniennes du nord-ouest du Nouveau-Brunswick. Geological Survey of Canada, Open File 4886, 109 p.

_____, Chagnon, A., Duchaine, Y., Lavoie, D., Malo, M. and Savard, M.M. 2003. Sedimentologic, diagenetic and tectonic evolution of the Saint-Flavien gas reservoir at the structural front of the Québec Appalachians. Bulletin of Canadian Petroleum Geology, v. 51, p. 126–154.

Bordet, E., Malo, M. and Kirkwood, D. 2006. Structural analysis of faults and fractures affecting the Lower Paleozoic margin of Anticosti, Québec Appalachians. The history of convergent and passive margins in the Polar realm. ILP task force on sedimentary basins, Québec 2006 meeting. Abstracts volume, p. 14.

_____, _____ and _____ (this issue). A structural study of western Anticosti Island, St. Lawrence platform, Quebec: a fracture analysis that integrates surface and subsurface structural data. Bulletin of Canadian Petroleum Geology, v. 58, no. 1, p. 36–55.

Bourque, P.-A. 2001. Sea-level, syn-sedimentary tectonics, and reefs: implications for hydrocarbon exploration in Silurian-Lowermost Devonian Gaspé Belt, Québec Appalachians. Bulletin of Canadian Petroleum Geology, v. 49, p. 217–237.

_____, Brisebois, D. and Malo, M. 1995. Gaspé Belt. In: Geology of the Appalachian/Caledonian Orogen in Canada and Greenland. H. Williams (ed.). Geological Society of America, Geology of North America, v. F-1, p. 316–351.

_____, Malo, M. and Kirkwood, D. 2001. Stratigraphy, tectono-sedimentary evolution and paleogeography of the post-Taconian B pre-Carboniferous Gaspé Belt: an overview. Bulletin of Canadian Petroleum Geology, v. 49, p. 186–201.

_____, Amyot, G., Desrochers, A., Gignac, H., Gosselin, C., Lachambre, G. and Laliberté, J.-Y. 1986. Silurian and Lower Devonian reefs and carbonate complexes of the Gaspé basin, Québec - a summary. Bulletin of Canadian Petroleum Geology, v. 34, p. 452–489.

Burden, E.T. and Williams, S.H. 1995. Biostratigraphy and thermal maturity of strata in Hunt-PanCanadian Port au Port #1 well. Public Access Well Report, Newfoundland Department of Mines and Energy, 95 p.

_____ and _____ 1996. Biostratigraphy and thermal maturity of strata in NHOC-PCP Long Point M16. Public Access Well Report, Newfoundland Department of Mines and Energy, 75 p.

Carter, T., Trevail, R. and Easton, R. 1996. Basement controls on some hydrocarbon traps in southern Ontario, Canada. In: Basement and basins of eastern North America. B.A. van der Pluijm and P.A. Catacosinos (eds.). Geological Society of America Special Paper 308, p. 95–107.

Castonguay, S., Wilson, R.A, Brisebois, D., Desrochers, A. and Malo, M. 2005. Compilation géologique, Anticosti–Gaspé-Campbellton, Les ponts géologiques de l'est du Canada, Transect 4, Québec - Nouveau-Brunswick. Geological Survey of Canada, Open File 4883, 1:125 000, 4 sheets.

Chi, G., Lavoie, D. and Salad Hersi. O. 2000. Dolostone units of the Beekmantown Group in the Montréal area, Québec: diagenesis and constraints on timing of hydrocarbon activities. Geological Survey of Canada, Current Research. 2000-D1, 8 p.

_____, _____ and Lynch, G. 2001. Petrographic and geochemical study of dolostones in the Trenton Formation from the Chaloupe Well, Anticosti Island, with comparison to dolostones of the Romaine Formation. Internal report to Shell Canada, 30 p.

_____,_____, Bertrand, R. and Lee, M.-K. (in press). Downward hydrocarbon migration predicted from numerical modeling of fluid overpressure in the Paleozoic Anticosti Basin, eastern Canada. Geofluids, v. 10. doi: 10.1111/j.1468-8123.2010.00280.x

Conliffe, J., Azmy, K., Knight, I. and Lavoie, D. 2009. Dolomitization in the Lower Ordovician Watts Bight Formation of the St Georges Group, Western Newfoundland. Canadian Journal of Earth Sciences, v. 46, p. 247–261.

Cooper, M., Weissenberger, J., Knight, I., Hostad, D., Gillespie, D., Williams, H., Burden, E., Porter-Chaudhry, J., Rae, D. and Clark, E. 2001. Basin evolution in western Newfoundland: new insights from hydrocarbon exploration. American Association of Petroleum Geologists Bulletin, v. 85, p. 393–418.

David, J. and Gariepy, C. 1990. Early Silurian orogenic andesites from the central Québec Appalachians. Canadian Journal of Earth Sciences, v. 27, p. 632–643.

_____, Chabot, N., Marcotte, C., Lajoie, J. and Lespérance, P.J. 1985. Stratigraphy and sedimentology of the Cabano, Pointe aux Trembles, and Lac Raymond formations, Témiscouata and Rimouski counties, Québec. Current Research, Geological Survey of Canada, Paper 85-1B, p. 491–497.

Davies, G. R. and Smith, L.B. 2006. Structurally controlled hydrothermal dolomite facies: an overview. Bulletin of the American Association of Petroleum Geologists, v. 90, p. 1641–1690.

Desaulniers, E. 2005. Imagerie sismique de la ligne 2002-MRN-10b: Recherche d'une approche géophysique au service de l'interprétation. M.Sc. thesis, Université Laval, Québec, 124 p.

Desrochers, A. 1985. The Lower and Middle Ordovician platform carbonates of the Mingan Islands, Québec: stratigraphy, sedimentalogy, paleokarst, and limestone diagenesis. Ph.D. thesis, Memorial University of Newfoundland, 454 p.

_____ and James, N.P. 1988. Early Paleozoic surface and subsurface paleokarst: Middle Ordovician Carbonates, Mingan Islands, Québec. In: Paleokarst. N.P. James and P.W. Choquette (eds.). Springer-Verlag, p. 183–210.

_____, Lavoie,. D., Brennan-Alpert, P. and Chi, G. (in press). Regional stratigraphic, depositional and diagenetic patterns from the interior of St. Lawrence Platform: the Lower Ordovician Romaine Formation, western Anticosti Basin, Québec. In: The Great American Carbonate Bank: The Geology and Petroleum Potential of the Cambro- Ordovician Sauk Sequence of Laurentia. J.R. Derby, R. Fritz, W. Morgan and C. Sternbach (eds.). American Association of Petroleum Geologists Memoir.

Dix, G.R. and Al Rodhan, Z. 2006. A new geological framework for the Middle Ordovician Carillon Formation (uppermost Beekmantown Group, Ottawa Embayment): onset of Taconic foreland deposition and tectonism within the Laurentian platform interior. Canadian Journal of Earth Sciences, v. 43, p. 1367–1387.

Dostal, J., Laurent, R. and Keppie, J.D. 1993. Late Silurian-Early Devonian rifting during dextral transpression in the southern Gaspé Peninsula (Québec): petrogenesis of volcanic rocks. Canadian Journal of Earth Sciences, v. 30, p. 2283–2294.

Doyon, M. 1988. Géochimie et environnement tectono-stratigraphique des roches volcaniques du centre nord de la Gaspésie, Québec. Ph.D. thesis, Université de Montréal, Montréal Canada, 254 p.

Friedman, I. and O'Neil, J.R. 1977. Compilation of stable isotope fractionation factors of geochemical interest. US Geological Survey Professional Paper 440 KK, 12 p.

Gasparrini, M., Bechstädt, T. and Boni, M. 2006. Massive hydrothermal dolomites in the southwestern Cantabrian Zone (Spain) and their relation to the Late Variscan evolution. Marine and Petroleum Geology, v. 23, p. 543–568.

Grevemeyer, I., Kaul, N., Diaz-Naveas, J.L., Villinger, H.W., Ranero, C.R. and Reichert, C. 2005. Heat flow and bending-related faulted at subduction trenches: case studies offshore of Nicaragua and Central Chile. Earth and Planetary Science Letters, v. 236, p. 238–248.

Harmon, R.S. and Hoefs, J. 1984. O-isotope relationships in Cenozoic volcanic rocks: evidence for a heterogeneous mantle source and open-system magma genesis. In: Proceedings of ISEM field conference on Open Magmatic System, p. 69–71.

Hepburn, J.C., Dunning, G.R. and Hon, R. 1995. Geochronology and regional tectonic implications of Silurian deformation in the Nashoba terrane, southeastern New England, USA. In: Current Perspectives in the Appalachian-Caledonian Orogen. J. Hibbard, C.R. van Staal and P. Cawood (eds.). Geological Association of Canada, Special Paper 41, p. 349–366.

Hurley, N.F. and Budros, R. 1990. Albion-Scipio and Stoney Point fields – USA Michigan Basin. In: Stratigraphic traps 1. E.A. Beaumont and N.H. Foster (eds.). American Association of Petroleum Geologists, Treatise of Petroleum Geology, Atlas of Oil and Gas fields, p. 1–38.

Jacobi, R.D. 1981. Peripheral bulge – a causal mechanism of the Lower/Middle Ordovician unconformity along the western margin of the northern Appalachians. Earth and Planetary Science Letters, v. 56, p. 245–251.

James, N.P., Stevens, R.K., Barnes, C.R. and Knight, I. 1989. Evolution of a Lower Paleozoic continental-margin carbonate platform, northern Canadian Appalachians. In: Controls on Carbonate Platform and Basin Development. P.D. Crevello, J.L. Wilson, J.F. Sarg, and J.F. Read (eds.). Society of Economic Paleontologists and Mineralogists, Special Publication 44, p. 123–146.

Kirkwood, D., Lavoie, M. and Marcil, J.S. 2004. Structural style and hydrocarbon potential in the Acadian Foreland Thrust and Fold Belt, Gaspé Appalachians, Canada. In: Deformation, Fluid Flow and Reservoir Appraisal in Foreland Fold and Thrust Belts. R. Swennen, F. Roure and J.W. Granath (eds.). American Association of Petroleum Geologist, Hedberg Series, no. 1, p. 412–430.

Knight, I., James, N.P. and Lane, T.E. 1991. The Ordovician St. George Unconformity, northern Appalachians: the relationship of plate convergence at the St. Lawrence Promontory to the Sauk-Tippecanoe sequence boundary. Geological Society of America Bulletin, v. 103, p. 1200–1225.

_____, Azmy, K., Greene, M. and Lavoie, D. 2007. Lithostratigraphic setting of diagenetic, isotopic, and geochemistry studies of Ibexian and Whiterockian carbonates of the St. George and Table Head groups in western Newfoundland. Current Research Newfoundland and Labrador Department of Natural Resources Geological Survey. Report 07-1, p. 55–84.

Kolata, D.R., Huff, W.D. and Bergström, S.M. 1996. Ordovician K-bentonites of eastern North America. Geological Society of America, Special Publication 313, 84 p.

Land, L. S. 1983. The application of stable isotopes to studies of the origin of dolomite and to problems of diagenesis of clastic sediments. In: Stable Isotopes in Sedimentary Geology. M. A. Arthur, T. F. Anderson, I. R. Kaplan, J. Veizer and L. S. Land (eds.). SEPM Short Course Notes 10, p. 4-1– 4-22.

Laurent, R. and Bélanger, J. 1984. Geochemistry of Silurian-Devonian alkaline basalt suites from the Gaspé Peninsula, Québec Appalachians. Maritime Sediments and Atlantic Geology, v. 20, p. 67–78.

Lavoie, D. 1988. Stratigraphie, sédimentologie et diagenèse du Wenlockien (Silurien) du bassin de Gaspésie - Matapédia. Unpublished Ph.D. thesis, Laval University, Québec, 330 p.

_____1994. Diachronous tectonic collapse of the Ordovician continental margin, eastern Canada: comparison between the Québec Reentrant and the St. Lawrence Promontory. Canadian Journal of Earth Sciences, v. 31, p. 1309–1319.

_____ 1997. The Romaine Formation in ARCO-NACP-LGCP wells (Anticosti Island), high-frequency cyclicity and significance for porosity. Confidential report to Shell Canada, 28 p.

_____ 1998. Porosity log for the Romaine Formation in the LGCP and NACP wells. Confidential report to Shell Canada, 10 p.

_____ 2006. Hydrocarbons in the Paleozoic basins of eastern Canada: new perspectives and promising targets. CSPG Technical Luncheon Talk, March 21, 2006. Canadian Society of Petroleum Geologists, Reservoir, v. 33, no. 2, p. 13.

_____ 2008. Appalachian Foreland Basin of Canada. In: Sedimentary Basins of the World - USA and Canada. A.D. Miall (ed.). Elsevier Science, The Netherlands, p. 65–103.

_____ and Bourque, P.-A. 1993. Marine, burial and meteoric diagenesis of Early Silurian carbonate ramps, Québec Appalachians, Canada. Journal of Sedimentary Petrology, v. 63, p. 233–247.

_____ and Chi, G. 2001. The Lower Silurian Sayabec Formation in northern Gaspé: carbonate diagenesis and reservoir potential. Bulletin of Canadian Petroleum Geology, v. 49, p. 282–298.

_____ and _____ 2006a. Lower and Middle Ordovician dolomites on Anticosti platform: contrasting patterns and fluid history. American Association of Petroleum Geologists, Annual Meeting of Eastern Section, Buffalo, 2006. Program with abstracts, p. 25–26.

_____and _____2006b. Hydrothermal dolomitization in the Lower Silurian La Vieille Formation in northern New Brunswick: geological context and significance for hydrocarbon exploration. Bulletin of Canadian Petroleum Geology, v. 54, p. 380–395.

_____ and Morin, C. 2004. Hydrothermal dolomitization in the Lower Silurian Sayabec Formation in northern Gaspé - Matapédia (Québec): constraint on timing of porosity and regional significance for hydrocarbon reservoirs. Bulletin of Canadian Petroleum Geology, v. 52, p. 256–269.

_____, Bourque, P.-A. and Héroux, Y. 1992. Early Silurian carbonate platforms in the Appalachian orogenic belt: the Sayabec - La Vieille formations of the Gaspé-Matapédia basin, Québec. Canadian Journal of Earth Sciences, v. 29, p. 704–719.

_____, Burden, E.T. and Lebel, D. 2003. Stratigraphic framework for the Cambrian-Ordovician rift and passive margin successions from southern Québec to western Newfoundland. Canadian Journal of Earth Sciences, v. 40, p. 177–205.

_____, Jackson, S. and Girard, I., 2010b. Mg Isotopes in high temperature saddle dolomites form the Lower Paleozoic of eastern Canada: significance for the source of Magnesium and their origin. American Association of Petroleum Geologists Annual Meeting New Orleans 2010, Program with abstracts.

_____, Chi, G., Brennan-Alpert, P., Desrochers, A. and Bertrand, R. 2005. Hydrothermal dolomitization in the Lower Ordovician Romaine Formation of the Anticosti Basin: significance for hydrocarbon exploration. Bulletin of Canadian Petroleum Geology, v. 53, p. 454–472.

_____, Dietrich, J., Pinet, N., Castonguay, S., Hannigan, P., Hamblin, T. and Giles, P.S. 2009. Hydrocarbon ressource assessment, Paleozoic basins of eastern Canada. Open File 6174, Geological Survey of Canada, 275 pages. http://geopub.nrcan.gc.ca/moreinfo_e.php?id=248071

_____, Chi, G., Urbastsch, M. and Davis, W.J. (2010a). Massive dolomitization if a pinnacle reef in Lower Devonian West Point Formation (Gaspé Peninsula, Québec): an extreme case of hydrothermal dolomitization through fault-focused circulation of magmatic fluids. American Association of Petroleum Geologists Bulletin, v. 94, no. 4, p. 513–531.

_____, Desrochers, A., Dix, G.R., Knight, I. and Salad-Hersi, O. (in press b). The Great American Carbonate Bank (GACB) in eastern Canada - an overview. In: The Great American Carbonate Bank: The Geology and Petroleum Potential of the Cambro- Ordovician Sauk Sequence of Laurentia. J.R. Derby, R. Fritz, W. Morgan, C. Sternbach, (eds.). American Association of Petroleum Geologists Memoir.

Long, D.G.F. 2007. Tempestite frequency curves: a key to Late Ordovician and Early Silurian subsidence, sea-level change, and orbital forcing in the Anticosti foreland basin, Québec, Canada. Canadian Journal of Earth Sciences, v. 44, p. 413–431.

Lonnee, J. and Machel, H.G. 2006. Pervasive dolomitization with subsequent hydrothermal alteration in the Clarke Lake gas field, Middle Devonian Slave Point Formation, British Columbia, Canada. Bulletin of American Association of Petroleum Geologists, v. 90, p. 1739–1761.

Lynch, G. 2000. Shell Canada – Encal Energy, Anticosti Island Exploration 1997–2000. Ministère des Ressources Naturelles et de la Faune du Québec, Report 2000TD456-01, 32 p., 47 figures.

_____ and Grist, A.M. 2002. Thermal modelling of the Laurentian margin beneath Anticosti Island using AFTA, 1D well profiles and bulk fluid inclusions. Canadian Society of Petroleum Geologists, Diamond Jubilee Convention. Program & Abstracts volume, p. 210.

Machel, H.G. and Lonnee, J. 2002. Hydrothermal dolomite – a product of poor definition and imagination. Sedimentary Geology, v. 152, p. 163–171.

Molgat, M. 2007. The petroleum system of Ontario: an overview in cores. 2007 CSPG-CSEG Convention, Core conference, Abstract on CD, p. 727.

Morin, C. and Laliberté, J.-Y. 2002. The unexpected Silurian-Devonian structural style in western Gaspé – new insight for promising hydrocarbon plays. Canadian Society of Petroleum Geology, Jubilee meeting, Calgary 2002, abstract volume, p. 240.

O'Brien, G.W., Lisk, M., Duddy, I.R., Hamilton, J., Woods, P. and Cowley, R. 1999. Plate convergence, foreland development and fault reactivation:

primary controls on brine migration, thermal histories and trap breach in the Timor Sea, Australia. Marine and Petroleum Geology, v. 16, p. 533–560.

Okubo, Y., Uchida, Y., Taniguchi, M., Miyakoshi, A. and Safanda, J. 2005. Statistical analysis for thermal data in the Japanese Islands. Physics of the Earth and Planetary Interiors, v. 152, p. 277–291.

Pinet, N. and Tremblay, A. 1995. Tectonic evolution of the Québec-Maine Appalachians: from oceanic spreading to obduction and collision in the northern Appalachians. American Journal of Science, v. 295, p. 173–200.

_____, Lavoie, D., Brouillette, P., Dion, D.J., Keating, P., Brisebois, D., Malo, M. and Castonguay, S. 2005. Gravimetric and aeromagnetic atlas of the Gaspé Peninsula. Geological Survey of Canada, Open File 5020, 68 p.

_____, _____, Keating, P. and Brouillette, P. 2008. Gaspé belt subsurface geometry in the northern Québec Appalachians as revealed by an integrated geophysical and geological study. 1- Potential field mapping. Tectonophysics, v. 460, p. 34–54.

Read, J.F. 1989. Controls on evolution of Cambrian-Ordovician passive margin, U.S. Appalachians. In: Controls on Carbonate Platform and Basin Development. P.D. Crevello, J.L. Wilson, J.F. Sarg and J.F. Read (eds.). Society of Economic Paleontologists and Mineralogists, Special Publication 44, p. 147–165.

Roy, S. 2004. Diagenèse et potentiel en hydrocarbures des successions paléozoïques de la region du Lac Matapédia, Québec. M.Sc. thesis, Institut National de la Recherche Scientifique – Eau, Terre et Environnement, Québec, Canada. 147 p.

_____ 2008. Maturation thermique et potentiel pétroligène de la Ceinture de Gaspé, Gaspésie, Québec, Canada. Ph.D. thesis, Institut National de la Recherche Scientifique – Eau, Terre et Environnement, Québec, Canada. 442 p.

Sacks, P.E., Malo, M., Trzcienski, W.E. Jr, Pincivy, A. and Gosselin, P. 2003. Taconian and Acadian transpression between the internal Humber Zone and the Gaspé Belt in the Gaspé Peninsula: tectonic history of the Shickshock Sud fault zone. Canadian Journal of Earth Sciences, v. 41, p. 635–653.

Sagan, J.A. and Hart, B.S. 2006. Three-dimensional seismic-based definition of fault-related porosity development: Trenton-Black River interval, Saybrook, Ohio. Bulletin of the American Association of Petroleum Geologists, v. 90, p. 1763–1785.

Salad Hersi, O. and Dix, G.R. 2006. Precambrian fault system as control on regional differences in relative sea level along the Early Ordovician platform of eastern North America. Journal of Sedimentary Research, v. 76, p. 700–716.

_____, Nowlan, G.S. and Lavoie, D. 2007. A revision of the stratigraphic nomenclature of the Cambrian-Ordovician strata of the Philipsburg tectonic slice, southern Québce. Canadian Journal of Earth Sciences, v. 44, p. 1775–1790.

Sanford, B.V. 1993. St. Lawrence Platform – Geology; Chapter 11. In: Sedimentary Cover of the Craton in Canada. D.F. Stott and J.D. Aitken (eds.). Geological Survey of Canada, Geology of Canada, no. 5, p. 723–786.

Shields, G.A., Carden, G.A.F., Veizer, J., Meidla, T., Rong, J.-Y. and Li, R-Y. 2003. Sr, C and O isotope geochemistry of Ordovician brachiopods: a major isotopic event around the Middle-Late Ordovician transition. Geochimica et Cosmochimica Acta, v. 67, p. 2005–2025.

Sibley, D.F. and Greg, J.M. 1987. Classification of dolomite rock textures. Journal of Sedimentary Petrology, v. 57, p. 967–975.

Sibson, R.H. 1990. Faulting and fluid flow. In: Fluids in tectonically active regimes of the continental crust. B.E. Nesbitt (ed.). Mineralogical Association of Canada Short Course Handbook, v. 18, p. 93–132.

_____ 2000. Fluid movement in normal faulting. Journal of Geodynamics, v. 29, p. 469–499.

Slater, B., Nyahay, R. and Smith, L.B. 2007. Outcrop analogue for hydrothermal dolomite reservoirs, Mohawk valley, New York. American Association of Petroleum Geologists, Annual Meeting Long Beach, 2007. Abstracts volume, p. 128.

Sloss, L.L. 1963. Sequences in the cratonic interior of North America. Geological Society of America Bulletin, v. 74, p. 93–114.

Smith, L. B. 2006. Origin and reservoir characteristics of Upper Ordovician Trenton-Black River hydrothermal dolomite reservoirs in New York, USA. Bulletin of the American Association of Petroleum Geologists, v. 90, p. 1691–1718.

Taylor, G.H., Teichmüller, M., Davis, A., Diessel, C.F.K., Littke, R. and Robert, P. 1998. Organic petrology, Berlin – Stuttgart, Gebrüder Borntraeger, 704 p.

Thomson, R.E., Subbotina, M.M. and Anisimov, M.V. 2005. Numerical simulation of hydrothermal vent-induced circulation at Endeavour Ridge. Journal of Geophysical Research C: Oceans, v. 110, p. 1–14.

Tremblay, A. and Pinet, N. 2005. Diachronous supracrustal extension in an intraplate setting and the origin of the Connecticut Valley-Gaspé and Merrimack troughs, northern Appalachians. Geological Magazine, v. 142, p. 7–22.

van Staal, C.R. 2005. The Northern Appalachians. In: Encyclopedia of Geology. R.C. Selley, L. Robin, M. Cocks and I.R. Plimer (eds.). Elsevier, Oxford, v. 4, p. 81–91.

_____ and de Roo, J.A. 1995. Mid-Paleozoic tectonic evolution of the Appalachian Central Mobile Belt in northern New Brunswick, Canada: collision, extensional collapse and dextral transpression. In: Current Perspectives in the Appalachian-Caledonian Orogen. J.P. Hibbard, C.R. van Staal and P.A. Cawood (eds.). Geological Association of Canada, Special Paper 41, p. 367–389.

_____, Ravenhurst, C.E., Winchester, J.A., Roddick, J.C. and Langton, J.P. 1990. Evidence for a post-Taconic blueschist suture in northern New Brunswick, Canada. Geology, v. 18, p. 1073–1077.

Walker, J., Gower, S. and McCutcheon, S.R. 1993. Antinouri Lake – Nicholas Denys Project, Gloucester and Restigouche counties, New Brunswick. In: Current Research. S.A. Abbott (ed.). New Brunswick Department of Natural Resources and Energy, Mineral Resources, Information Circular 93-1, p. 58–70.

Wierzbicki, R., Dravis, J.J., Al-Aasm, I. and Harland, N. 2006. Burial dolomitization and dissolution of the Upper Jurassic Abenaki platform carbonates, Deep Panuke reservoir, Nova Scotia, Canada. Bulletin of American Association of Petroleum Geologists, v. 90, p. 1843–1861.

Wilson, E.N., Hardie, L.A. and Phillips, O.M. 1990. Dolomitization front geometry, fluid flow patterns and the origin of massive dolomite: the Triassic Latemar build-ups, northern Italy. American Journal of Science, v. 290, p. 741–796.

Wilson, R.A. 1992. Petrographic features of Siluro-Devonian felsic volcanic rocks in the Riley Brook area, Tobique Zone, New Brunswick: implications for base metal mineralization at Sewell Brook. Atlantic Geology, v. 28, p. 115–135.

_____, Burden, E.T., Bertrand, R., Asselin, E. and McCracken, A.D. 2004. Stratigraphy and tectono-sedimentary evolution of the Late Ordovician to Middle Devonian Gaspé Belt in northern New Brunswick: evidence from the Restigouche area. Canadian Journal of Earth Sciences, v. 41, p. 527–551.

Date accepted: March 4, 2010

Associate Editor: Kirk Osadetz